UNIVERSITA' DEGLI STUDI DI PADOVA

Sede Amministrativa: Università degli Studi di Padova

Dipartimento di Scienze biomediche sperimentali

SCUOLA DI DOTTORATO DI RICERCA IN BIOSCIENZE

INDIRIZZO: BIOLOGIA CELLULARE

CICLO XXI

Ca^{2+} HOMEOSTASIS IN MAMMALIAN AND PLANT PEROXISOMES

Direttore della Scuola: Ch.mo Prof. Tullio Pozzan

Supervisore: Ch.mo Prof. Tullio Pozzan

Dottorando: Ilaria Drago

INDEX

SUMMARY

Peroxisomes are single-membrane bound organelles involved in reactive oxygen species scavenging, α- and β-oxidation of fatty acids, biosynthesis of ether phospholipids and other metabolic pathways. Although recent studies have highlighted the mechanisms of peroxisomal formation, fusion-fission, protein import etc. little information is available concerning a possible role of peroxisomes in cellular signalling, and, until very recently, no information was available about a possible role of peroxisomes in cellular Ca^{2+} handling. Ca^{2+} signalling exerts a plethora of functions in cells (both in physiology and pathology) and while the role of subcellular compartments like endoplasmic reticulum, mitochondria, nucleus and Golgi apparatus in Ca^{2+} handling has been intensively investigated in the last decades, peroxisomes remained a black whole in the picture. Last, but not least, a renewed interest towards peroxisome functions has been triggered by the discovery of a number of human diseases (called "peroxisomal disorders") that are due to mutations of peroxisomal proteins. For all these reasons, I decided to investigate if and how peroxisomes play a role in cellular Ca^{2+} handling.

I targeted a genetically encoded, FRET-based Ca^{2+} sensor to peroxisomal matrix and I found that the Ca^{2+} concentration of peroxisomes in living cells at rest is similar to that of the cytosol, while increases in cytosolic Ca^{2+} concentration (elicited by either Ca^{2+} mobilization from stores or Ca^{2+} influx through plasma membrane Ca^{2+} channels) are usually followed by a slow rise in intraperoxisomal Ca^{2+} concentration. I also investigated the mechanism of peroxisomal Ca^{2+} entry and I found that Ca^{2+} influx into peroxisomes is not driven by an ATP-dependent pump, membrane potential or H^+ (Na^+) gradients. However, the peroxisomal membrane appears to play a low-pass filter role, preventing the organelle from taking up Ca^{2+} during short lasting cytosolic Ca^{2+} transients, while allowing equilibration of the peroxisomal luminal Ca^{2+} concentration with that of the cytosol during prolonged cytosolic Ca^{2+} increases. Thus, peroxisomes appear to be an additional cytosolic Ca^{2+} buffer, but their influx and efflux mechanisms are unlike those of any other cellular organelle.

The second part of my work was aimed at understanding the physiological function of this phenomenon. To date, no Ca^{2+}-regulated mammalian peroxisomal enzyme is known. On the contrary, there are some Ca^{2+}-regulated plant peroxisomal enzymes, in particular an isoform of the H_2O_2 scavenging enzyme catalase, Cat3. Cat3 has been shown to be specifically located in plant peroxisomes and to be activated *in vitro* by Ca^{2+} and calmodulin.

The peroxisomal Ca^{2+} probe employed in the first part of this work was expressed in plant peroxisomes and revealed that the phenomenon of Ca^{2+} entry into peroxisomal matrix in plants is very similar, both in amplitude and kinetic, to that of mammalian cells. Plasma membrane hyperpolarization demonstrated to be a reliable stimulus to trigger a prolonged rise of peroxisomal (and cytosolic) Ca^{2+} concentration and so it was chosen in order to verify if a peroxisomal Ca^{2+} rise can somehow affect H_2O_2 scavenging. Preliminary experiments performed in *Arabidopsis* plants stably expressing in peroxisomes a H_2O_2 sensor indicate that H_2O_2 scavenging is accelerated by Ca^{2+} entry and this is correlated with the level of Cat3 within peroxisomes.

RIASSUNTO

I perossisomi sono degli organelli intracellulari circondati da una singola membrana coinvolti nell'eliminazione di specie reattive dell'ossigeno, α- e β-ossidazione di acidi grassi, biosintesi di eteri di fosfolipidi e in altre reazioni metaboliche. Sebbene studi recenti abbiano elucidato i meccanismi alla base della formazione, della fusione- fissione e dell'importo di proteine nella matrice dei perossisomi, le informazioni riguardanti il ruolo dei perossisomi nel *signalling* cellulare sono scarse e, fino a poco tempo fa, quelle riguardanti il possibile ruolo dei perossisomi nel *signalling* cellulare del Ca^{2+} erano totalmente assenti.

Il *signalling* del Ca^{2+} è alla base di un ampio numero di funzioni cellulari sia fisiologiche che patologiche e mentre il ruolo di compartimenti subcellulari come il reticolo endoplasmico, i mitocondri, il nucleo e l'apparato di Golgi nelle dinamiche intracellulari del Ca^{2+} è stato ampiamente studiato negli ultimi decenni, i perossisomi sono rimasti nella "zona d'ombra" di questo scenario. Infine, c'è stato ultimamente un rinnovato interesse circa le funzioni dei perossisomi grazie alla scoperta di un certo numero di malattie umane (chiamate "disordini dei perossisomi") dovute a mutazioni di proteine perossisomiali.

Per tutte queste ragioni, ho deciso di investigare se, e come, i perossisomi rivestono un qualche ruolo nell'omeostasi intracellulare del Ca^{2+}.

A questo scopo ho indirizzato alla matrice dei perossisomi una sonda per il Ca^{2+} geneticamente codificata e basata su FRET e ho potuto dimostrare che la concentrazione di Ca^{2+} nei perossisomi di cellule vive in condizioni di riposo è molto simile a quella citosolica mentre aumenti della concentrazione di Ca^{2+} (causati sia da mobilizzazione di Ca^{2+} dai depositi intracellulari che da influsso attraverso canali per il Ca^{2+} situati nella membrana plasmatica) sono solitamente seguiti da un lento aumento della concentrazione di Ca^{2+} nella matrice perossisomiale.

Mi sono inoltre occupata della caratterizzazione del meccanismo che sta alla base dell'entrata di Ca^{2+} nei perossisomi e sono arrivata alla conclusione che questo fenomeno non è dovuto alla presenza di una pompa dipendente da ATP, né di un potenziale di membrana o di un gradiente di H^+ o Na^+. La membrana dei perossisomi sembra costituire una barriera che previene l'entrata di Ca^{2+} nel caso di aumenti brevi nel tempo, mentre nel caso di aumenti prolungati della concentrazione di Ca^{2+} nel citosol permette una lenta equilibrazione della concentrazione di Ca^{2+} nella matrice perossisomiale con l'ambiente citosolico. I perossisomi sembrano quindi costituire un nuovo sistema-tampone per il Ca^{2+}del citosol, sebbene il loro

meccanismo di influsso ed efflusso per il Ca^{2+} è totalmente differente da quello di ogni altro organello cellulare.

La seconda parte del mio lavoro si è poi concentrata sullo studio dei possibili ruoli fisiologici del fenomeno dell'entrata di Ca^{2+} nei perossisomi. In letteratura non sono al momento riportati degli enzimi localizzati nei perossisomi delle cellule di mammifero che siano regolati da Ca^{2+}; al contrario, alcuni enzimi localizzati nei perossisomi delle piante sembrano essere regolati da Ca^{2+}. Di questi, quello che più mi è sembrato interessante è un'isoforma di un enzima deputato all'eliminazione di H_2O_2, la catalasi. L'attività di Cat3 è infatti riportata essere attivata *in vitro* da Ca^{2+} e calmodulina. La sonda per il Ca^{2+} utilizzata per lo studio dei perossisomi in cellule di mammifero è stata quindi indirizzata ai perossisomi di cellule vegetali e ha permesso di dimostrare che il fenomeno dell'entrata di Ca^{2+} nei perossisomi è molto simile, sia per ampiezza che per cinetica, tra perossisomi di mammifero e di pianta. L'iperpolarizzazione della membrana plasmatica ha dimostrato essere uno stimolo ripetibile che causa un prolungato aumento della concentrazione di Ca^{2+} nei perossisomi (e nel citosol) di pianta ed è quindi stato scelto per verificare se un aumento di Ca^{2+} nei perossisomi possa in qualche modo influenzare l'eliminazione di H_2O_2.

Esperimenti preliminari effettuati in piante di *Arabidopsis* che esprimono stabilmente una sonda per H_2O_2 geneticamente codificata indicano che l'eliminazione di H_2O_2 è notevolmente accelerata in seguito all'entrata di Ca^{2+}; questo correla con il livello di Cat3 espressa nei perossisomi.

PART I

Ca^{2+} HOMEOSTASIS IN MAMMALIAN PEROXISOMES

INTRODUCTION

1. PEROXISOMES

Peroxisomes are single-membrane bound organelles found in all eukaryotes except the Archaezoa. They were first described by Rhodin in 1954 and then biochemically characterized by DeDuve in 1966. Although at that time they were considered as the "Cinderella" among the subcellular compartments, in very few years the list of biological functions attributed to peroxisomes has grown substantially and they are now known to be fundamental for many cell functions (Shrader and Fahimi, 2008).

Peroxisomes carry out diverse metabolic activities, like β-oxidation of lipid molecules and detoxification of reactive oxygen species, and exhibit high metabolic plasticity, as their enzymatic content can vary depending on environmental condition, tissue or cell type. The importance of peroxisomes in multi-cellular organisms is also reflected by the severe phenotypes characterizing human diseases due to impairment in peroxisomes formation and maintenance or due to the absence or reduction of one of the enzymatic activities housed within their matrix (Titorenko and Rachubinski, 2004).

1.1 Peroxisome biogenesis, maintenance and inheritance

The study of peroxisomal biogenesis, maintenance and inheritance was very difficult due to the extreme fragility and low abundance of this organelle; however, genetic screens, first in yeast and then in Chinese hamster ovary cells and *Arabidopsis thaliana* have identified 32 evolutionary conserved genes whose products are needed for peroxisomal assembly (Fujiki et al., 2006; Nito et al., 2007; Wolinski et al., 2009). They are called PEX genes and their products peroxins, and they are involved in three different processes: i) import of peroxisomal matrix proteins; ii) membrane biogenesis and iii) organelle proliferation.

The duplication of pre-existing peroxisomes by fission and subsequent growth and maturation is the major pathway of proliferation. The peroxisome fission process is not fully understood, however, though it is now accepted that it is based on specific peroxisomal proteins, like Pex11p, and on some other components shared with the mitochondrial fission machinery, e.g. the dynamin-like protein DLP1 and Fis1p (Fig. 1.1). The peroxisomal membrane proteins Pex11p, Pex25p and Pex27p contribute to the elongation and constriction

of mature peroxisomes; after this process, peroxisomes undergo fission thanks to DLP1 that is anchored to the peroxisomal membrane by Fis1p. At the end of the process, Pex28p and Pex29p control separation of divided, but yet clustered, peroxisomes (Platta and Erdmann, 2007).

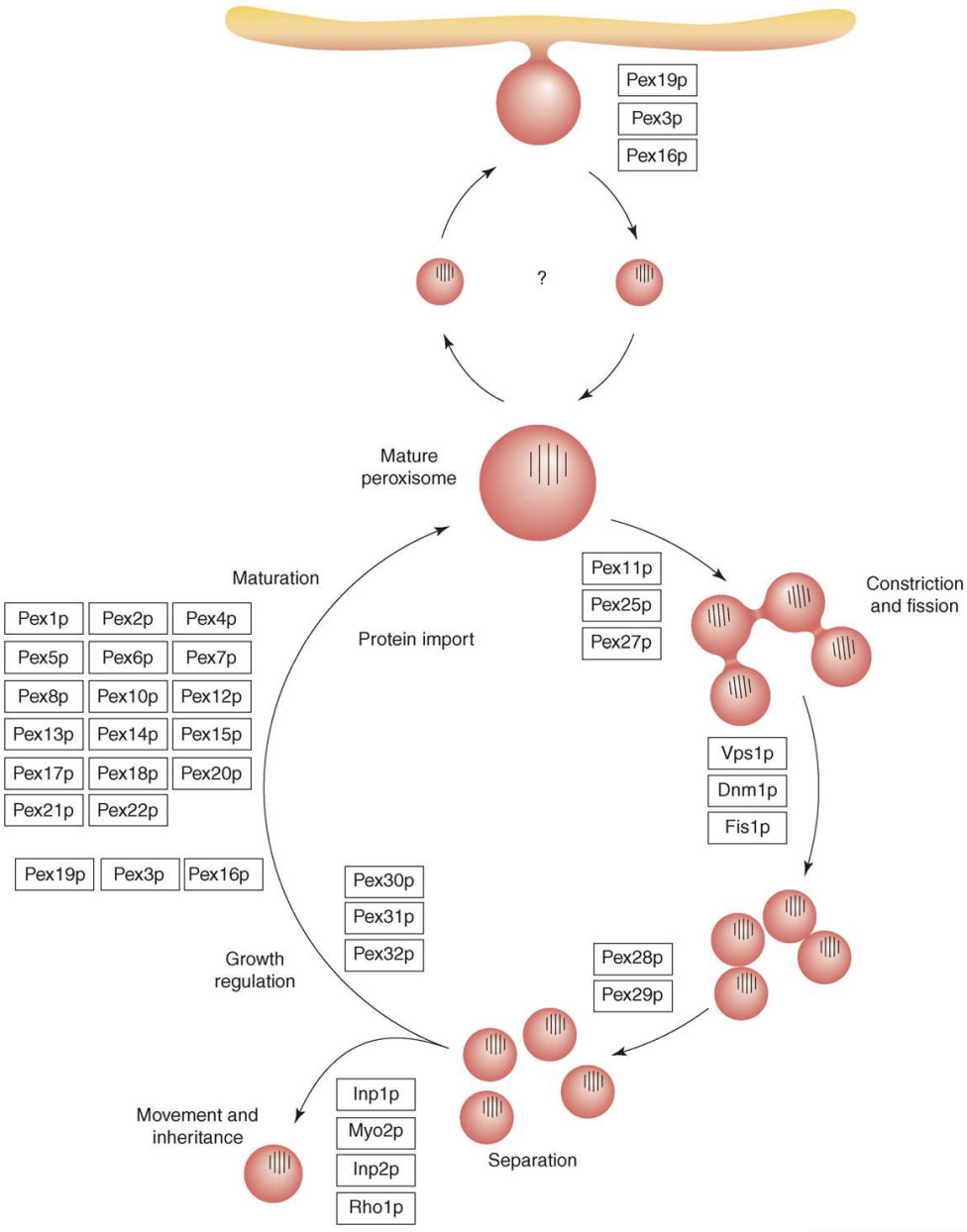

Figure 1.1. Schematic overview of proteins involved in peroxisomal proliferation and dynamic. Peroxisomes can be generated either by *de novo* formation from ER or by fission of pre-existing peroxisomes. Maturation of peroxisomes involves import of proteins from cytosol or sorted through endoplasmic reticulum. See § 1.1 for details. Adapted from Platta and Erdmann, 2007.

The size of peroxisomes is then tightly dependent on the import of matrix proteins, whose rate of production is controlled by peroxisome proliferators-activated receptor α (PPAR α), a member of the family of ligand-activated nuclear transcription factors (Kliewer et al., 1992). It is activated by lipid ligands and it controls the transcription of several peroxisomal genes, particularly those involved in peroxisome proliferation and lipid metabolism.

In addition to the process of duplication from pre-existing peroxisomes, a few years ago the work by Hoepfner et al. demonstrated that the endoplasmic reticulum (ER) contributes significantly to peroxisome biogenesis. In an elegant series of experiments, they demonstrated that the peroxin Pex3p targets the ER membrane and then concentrates in "dots"; from these dots, thanks to the activity of Pex19p, pre-peroxisomes are formed by budding and these vescicles in turn import peroxisomal membrane and matrix proteins, becoming mature peroxisomes (Hoepfner et al., 2005). Based on these findings, peroxisomes are now considered to be part of the secretory pathway, although the relative importance of *de novo* formation from ER *vs* fission from pre-existing peroxisomes is still matter of debate (van der Zand et al., 2006).

As reported for other organelles, inheritance of peroxisomes is not random, but it is strictly controlled. In *S. Cerevisiae* Inp1p, which anchors peroxisomes to cellular cortex, the myosin Myo2p and the GTPase Rho1p were identified as members of this process. In mammalian cells, although it is clear that peroxisomes move along microtubules in a well-controlled manner, proteins involved remain to be identified (Platta and Erdmann, 2007).

1.2 Peroxisomal matrix protein import

Peroxisomes do not possess their own DNA and do not have their protein translation machinery, like mitochondria and chloroplast, and all the proteins they need are encoded by nuclear genome. Their protein import mechanism differs from that of all other subcellular compartments: the majority of peroxisomal proteins are translated on free polyribosomes and then imported into peroxisomal matrix as folded, co-factor bound proteins (Leon et al., 2006). This process can be schematically divided into four steps (Fig. 1.2): i) cargo binding; ii) receptor-cargo docking to the peroxisome membrane; iii) receptor-cargo translocation and cargo release and iv) dislocation and recycling of the receptor.

1.2.1 Cargo binding

Peroxisomal proteins are synthesized in the cytosol and then they are transported into peroximal matrix via the recognition of one of two specific targeting signals. The most common peroxisomal targeting signal, named PTS1, is located at the carboxyl-terminal of the protein and is represented by the consensus sequence (S/A/C) (K/R/H) (L/M). Even if the most common PTS1 is SKL, different bioinformatics studies have demonstrated that this sequence can vary and, in order to be recognized by its receptor, the aminoacids that precede the tripeptide are critical for effective peroxisomal import (Neuberger et al., 2003). PTS1 is recognized by a cytosolic protein, Pex5p, which is composed by two main domains. The carboxy-terminal one is made up by seven tetratricopeptide repeats (TRP) and a helix bundle, which upon PTS1 binding form a ring-like structure. The amino-terminal domain is less conserved than the carboxy-terminal, and contains the peptide WXXXF/Y that appears necessary for peroxisomal targeting of the receptor-cargo complex.

The second peroxisomal targeting signal, PTS2, is less common and is represented by the consensus peptide RLXXXXX(H/Q)L located at the amino-terminus of the protein. The cytosolic receptor for this targeting peptide is Pex7p, whose predicted structure is that of a seven-bladed β-propeller domain. In mammals, there are two splice variants of PEX5 gene, a longer (PEX5L) and a smaller one (PEX5S). While PTS1-containing proteins need only Pex5p to be targeted into peroxisomes, PTS2 containing proteins, after recognition of their amino-terminal consensus peptide by Pex7p, need also Pex5lp in order to be transported into the peroxisomal matrix (Brown and Baker, 2008).

Thanks to the ability of this system to carry into peroxisomes folded and even oligomeric proteins, a PTS-containing subunit in a heterodimer can mediate the transport of other matrix proteins in a “piggy back” fashion, even if these proteins do not contain a PTS (Titorenko et al., 2002). The insertion of proteins located into the peroxisomal membrane (PMP) is less characterized. PMP are divided into two classes: PMP I and II. Class I PMPs are synthesized on free cytosolic ribosomes, subsequently they are traslocated to peroxisomal membrane thanks to an internal consensus sequence, named mPTS. This process is controlled by Pex19p that recognises mPTS, Pex3p, which serves as a membrane recruitment factor and by Pex16p that functions as Pex3p docking site in peroxisomal membrane (Matsuzaki and Fujiki, 2008). Class PMP II import on the contrary is Pex19p and Pex3p-independent.

1.2.2 Receptor-cargo docking to the peroxisome membrane

After PTS-bearing protein recognition in cytosol, the cargo-receptor complex interacts with the outer peroxisomal membrane thanks to a protein complex composed of Pex13p, Pex14p and also Pex17p in *S. Cerevisiae*. Pex13p is an integral membrane protein that, thanks to a Src-homology domain, can bind the PTS1 receptor Pex5p.

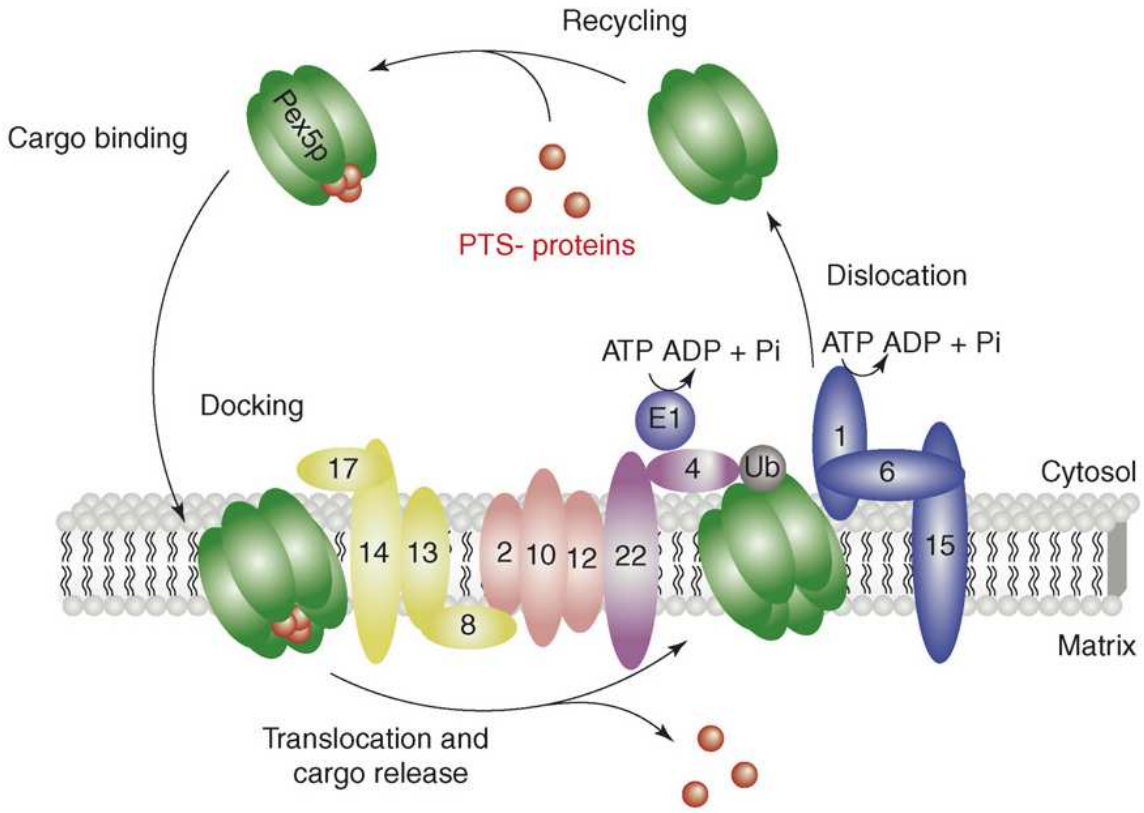

Figure 1.2. Protein import into peroxisomal matrix. The process, mediated in different organism by 32 proteins called peroxins, can be divided into four step: cargo binding, docking to the peroxisome membrane, translocation and cargo release and dislocation. PTS-proteins: peroxisome-targeting signal containing proteins; Ub, ubiquitine. Adapted from Platta and Erdmann, 2007.

The docking complex, in addition to bind the receptor-cargo protein complex, contributes to the assembly and stabilization of the translocon that mediates receptor-cargo entry into peroxisome matrix.

1.2.3 Receptor-cargo translocation and cargo release

In the translocation step the PTS-receptor is peroxisome associated and protease resistant, and, based on these two experimental observations, two different hypothesis have been proposed: i) extended shuttle hypothesis: the receptor-cargo complex enters into peroxisomal matrix; ii) simple shuttle hypothesis: the complex is embedded in the membrane, the receptor exposes its cargo binding site into the peroxisomal matrix and then release its cargo (Brown and Baker, 2008). In this process, the matrix-located peroxin Pex8p is required for the connection between the docking complex and the RING-finger complex, made of Pex2p, 10p and 12p. This complex is also called "importomer" although the mechanism by which the translocation takes place is far from understood.

1.2.4 Dislocation and recycling of the receptor

Protein import into peroxisomal matrix does not require ATP, whereas the export of Pex5p back to cytosol does (Oliveira et al., 2003). This process involves the peroxins Pex15p (and its homolog Pex26p in mammalian cells), Pex1p and Pex6p, and it needs also the presence of an ubiquitin-conjugating enzyme, Pex4p. This process takes place in the peroxisomal membrane and is part of a "quality control" system: a single ubiquitination targets Pex5p for recycling, while a polyubiquitination targets dysfunctional PTS receptors to degradation. This mechanism appears to be conserved also for PTS2 receptors. Another step that requires ATP is, at the end of the process, the detachment of the ubiquitinated receptor from the peroxisomal membrane, and it is mediated by Pex1p and Pex16p.

1.3 Peroxisome metabolic activities

Mammalian peroxisomes house up to fifty different enzymatic activities, many of them unique to peroxisomes, while others are shared with cytosol, mitochondria or both (Wanders and Waterham, 2006). The principal enzymatic reactions associated to peroxisomes are listed below.

i. **Oxygen metabolism:** peroxisomes possess oxidases that reduce O_2 to H_2O_2 that in turn is eliminated by different scavenging enzymes, like catalase, gluthatione peroxidase and peroxiredoxin V (Shrader and Fahimi, 2006). Peroxisomal enzymatic activities can also generate other reactive oxygen species than H_2O_2, e.g, superoxide anions, that can be inactivated by superoxide dismutase. Peroxisomes also contain epoxide hydrolase activity. This allows peroxisomes to

eliminate a group of highly reactive molecules, responsible for mutagenic activity, generated both endogenously and exogenously, and able to react with lipids containing unsaturated fatty acids, DNA, RNA and proteins. Finally, peroxisomes contain Glutatione S-transferase activity.

ii. **Ether-phospholipids biosynthesis:** the physiological role of ether phospholipids, including plasmalogens, is not well understood. Some evidence points to a role in membrane dynamics, intracellular signalling, cholesterol transport and metabolism, oxidative stress and polyunsaturated fatty acids metabolism (Titorenko and Rachubinski, 2004). In mammalian cells, the first two steps of plasmalogen biosynthesis occur exclusively into peroxisomes. This molecule, which makes up 18% of total phospholipid mass, has a cell and tissue specific distribution, being particularly abundant in nervous tissue and central white matter. This in part explains the severe developmental delay that characterizes patients with impaired plasmalogen biosynthesis, that in turn causes incomplete migration and differentiation of neuroblast and defects in the development of central white matter.

iii. **Fatty acids β-oxidation:** peroxisome enzymatic activities can vary upon different organism and cell types, but fatty acids β-oxidation is an exception to this rule. In yeast and plants, peroxisomes are the unique site of this reaction, while in mammals it can took place also in mitochondria. Although similar in mechanism, peroxisomal and mitochondrial fatty acids β-oxidation have different substrate specialization. Short and medium chain fatty acids are exclusively and long-chain fatty acids are predominantly oxidized in mitochondria, whereas very long fatty acids, that is, more than 26:0, can be oxidized only by peroxisomes. This is also the case of certain polyunsaturated fatty acids, certain prostaglandins, leukotrienes, some xenobiotics, vitamin K and E.

iv. **Peroxisomal fatty acids α-oxidation:** this reaction is necessary in order to obtain substrates for β-oxidation from fatty acids that carry a methyl group at the carbon 3 position. This reaction can took place only in peroxisomes, in contrast with β-oxidation.

v. **Amino acid catabolism:** mammalian peroxisomes, thanks to D-aminoacid oxidase, can oxidize D-isomers of neutral and basic aminoacid, while D-aspartate oxidase can perform the same reaction on acidic aminoacids. This reaction

produces the corresponding ketoacids, ammonia and hydrogen peroxide. Peroxisomes can also catabolize some L-aminoacids.

1.4 Peroxisomal metabolite transport and ionic concentration

Although the idea that peroxisomal function must be liked to a system that allows metabolite transport across the peroxisomal membrane is widely accepted, its study has proven difficult due to the fact that after isolation peroxisomal membrane is freely permeable to low molecular weight compounds. This fact led to the assumption that peroxisomal membrane does not constitute a permeability barrier to small molecules, at least in mammals. However, recent studies have proven that this is not true, since peroxisomal membrane is impermeable to small metabolites and is equipped with different carriers (Wanders and Waterham, 2006).

Mammalian peroxisomes have four different ABC transporters, adenoleukodistrophy protein (ALDP or ABCD1), ALDRP (or ABCD2), PMP70 (or ABCD3) and PMP70R (or ABCD4). These proteins belong to a family of proteins that couple ATP hydrolysis to metabolite transport and they function as homodimers and, likely, as heterodimers. Their function in peroxisomes is not characterized, even if the study of a human disease caused by ALDP mutation suggests that this protein is involved in very-long fatty acids β-oxidation.

The best characterized peroxisomal membrane protein is Ant1p and its orthologue in mammals PMP34, which provides intraperoxisomal ATP by catalyzing the nucleotide transport. It is not clear whether intraperoxisome ATP is necessary only for enzymatic reactions and cargo release or whether it serves as energy source for maintenance of ion gradients as well.

There is no general consensus about the pH gradient across peroxisomal membrane and, if it exists, how it is generated and maintained. While Dansen et al. (Dansen et al., 2000) in human fibroblast and van Roermund et al. in yeast measured a basic intraperoxisomal pH (van Roermund et al., 2004), Lasorsa et al. came to the opposite conclusion, i.e they concluded that peroxisome pH is slightly acidic in yeast (Lasorsa et al., 2004); finally Jankowski et al. found that mammalian peroxisomal pH is in equilibrium with cytosolic pH and no significant gradient exist between the two compartments (Jankowski et al, 2001).

1.5 Human peroxisomal disorders

The study of human peroxisomal genetic disorders has contributed to the understanding of the fundamental role of this organelle in normal mammalian development and growth. Peroxisomal disorders are classified into two groups, Peroxisomal Biogenesis Disorders (PBD) and single enzyme deficiencies.

The Zellweger syndrome (ZS) is the most common and severe disease belonging to the first class of peroxisomal diseases and is characterized by the compete absence of peroxisomes (Steinberg et al., 2006). This is due to mutations in one of 12 different PEX genes and results in accumulation of substrates usually handled by peroxisomes, e.g. very-long fatty acids, and in the absence of molecules, e.g. plasmalogens, produced by some peroxisomal enzymes that can not work in the cytosol (Santos et al., 1988). This in turn causes a global developmental delay, craniofacial and eye abnormalities, neuronal migration impairment, hepatomegaly. The affected patients usually die in the first year of life. Mutations in PEX7, that codes for PTS2 receptor and so affects only PTS2-bearing peroxisomal proteins targeting, cause rhizomelic chondrodysplasia punctata type 1, characterized by mental retardation, proximal bone shortening and severe growth deficiencies, but no neuronal migration defect like others PBD (Braverman et al., 1997).

Most peroxisomal disorders belong to the class of single enzyme deficiencies, where the patient phenotype severity is strictly dependent on the peroxisomal function that is impaired (Wanders and Waterham, 2006b). For example, in X-linked adrenoleukodistrophy, caused by an ALDP mutation (Mosser et al., 1993), there is an accumulation of very-long fatty acids in fibroblasts, other cell types and in plasma. In Refsum disease, fatty acids α-oxidation is impaired due to mutations in phytanoil-CoA hydrolase, resulting in phytanic acid plasma accumulation (Hutton and Steimberg, 1973). This disease is characterized by a late onset, starting in childhood with progressive deterioration of night vision, followed by retinitis pigmentosa, deafness, polyneurophathy and cardiac arrhythmias.

2. CELLULAR Ca^{2+} HOMEOSTASIS

In order to adapt to changing environments cells have developed a complex signal system based on messengers whose concentration changes both in time and space. Originally, cells began to exclude Ca^{2+} from cytoplasm due to its ability to precipitate phosphate; later the energy spent by cells to exclude this ion was used to trigger signal transduction (Clapham 2007). Cells maintain a steep Ca^{2+} gradient across plasma membrane: in cytoplasm there is a Ca^{2+} concentration ($[Ca^{2+}]c$) of ~100 nM, compared to an extracellular millimolar concentration. Small changes in intracellular $[Ca^{2+}]$ ($[Ca^{2+}]i$) (caused by Ca^{2+} influx from the extracellular medium or release from intracellular stores, see below) can trigger different cellular events, ranging from exocytosis to muscle contraction, fertilization and transcription activation (Fig. 2.1). Ca^{2+} cannot be chemically altered and accordingly, in order to strictly control its levels in the cytosol, cells have developed different systems to extrude, bind or compartimentalize it. The Ca^{2+} signalling toolkit is therefore based on protein that can bind it, systems that extrude it from cytoplasm or lead it into cells and into different subcellular compartments that can function as intracellular Ca^{2+} stores.

2.1 Ca^{2+} binding proteins

Many different Ca^{2+} binding proteins exist and their affinity for Ca^{2+} can vary from nM to mM. The best know protein domain able to specifically bind Ca^{2+} is the so called “EF hand domain”, present in hundreds of proteins. This domain is made up of a “helix turn helix” peptide, where several negatively charged oxygen atoms can coordinate Ca^{2+} in a 12 amino acids group (turn) between two orthogonal α-helices. EF domains can display very different Ca^{2+} affinities depending on mutations in amino acids belonging to the Ca^{2+} binding loop or to the side α-helices. The best known example among Ca^{2+} binding proteins is that of calmodulin (CaM), the ubiquitous Ca^{2+} sensor and adaptor protein that contains four EF hand domains. CaM has been highly conserved during evolution, indicating its essential function in all eukaryotes. It is made up of a central α-helix and at its end there are four EF hand domains, two at each side. Upon Ca^{2+} binding, there is a conformational change causing the exposure of a hydrophobic surface that in turn allows CaM to interact with the amphipatic regions of target proteins, thus modifying their activities (Hoeflich and Ikura, 2002).

Other cellular proteins that sense Ca^{2+} are S100 proteins, also endowed with EF hand domains. A distinct Ca^{2+} binding motif is the C2 domain, where a binding of two or three

Ca^{2+} ions cause protein's association with a specific region of cellular membranes (Donato, 1999). Cells are also endowed with proteins that function exclusively as Ca^{2+} buffers, in either the cytosol or within organelles. These proteins differ both for their Ca^{2+} affinity and speed of Ca^{2+} binding. Some examples of cytoplasmic Ca^{2+} buffers are parvalbumin, calbindin and calretinin; typical Ca^{2+} buffers present in the lumen of organelles are calreticulin (within the ER lumen) and calsequestrin (within the sarcoplasmic reticulum terminal cysternae) (Clapham 2007).

2.2 Pathways leading Ca^{2+} into cells

A cytosolic Ca^{2+} elevation can trigger a fast activation of different signalling pathways. These elevations can be due to the opening of Ca^{2+} channels, located in the plasma membrane or organelles, and allow Ca^{2+} to flow down its electrochemical gradient. Most ion channels are gated, i.e. capable of making transitions between conducting and non-conducting conformations. Gating of ion channels depends on different stimuli, being of either electrical or chemical nature. Depending on the activation mechanism, Ca^{2+} channels have generally been classified in voltage-gated and ligand-gated channels (Piertrobon et al., 1990; Fasolato et al., 1994).

2.2.1 Voltage-Operated Ca^{2+} Channels

Voltage-operated Ca^{2+} channels (VOCCs) can open upon plasma membrane depolarization and so they transform electrical signals into chemical signals. In the nervous system they control a broad array of functions including neurotransmitter release, neurite outgrowth, synaptogenesis, neuronal excitability, differentiation, plasticity, etc. VOCCs are multi-subunit complexes made up of a pore-forming and voltage-sensing $\alpha 1$ subunit and several auxiliary subunits, including 2δ and β subunits and, in some cases, also γ subunits. They constitute a complex family of channels comprising a large number of different subtypes, which have in common a steep voltage dependence of the open probability and a very high selectivity for Ca^{2+} over Na^{+} and K^{+} ions in physiological solution (Catterall and Few, 2008). They are located in the plasma membrane of excitable cells, e.g. in neurons, striated and (most smooth) muscles and neurosecretory cells, and are classified in different subtypes depending on voltage and inhibitors sensitivity in L-, N-, T-, P/Q-, and R- type.

2.2.2 Ligand-gated Ca^{2+} channels

Ligand-gated Ca^{2+} channels are characterized by a lower selectivity for Ca^{2+} over other monovalent cations if compared to VOCCs. This family of Ca^{2+} channels is usually divided into four subgroups:

i. **Receptor- Operated Ca^{2+} channels:** these channels possess a ligand-binding site in the same polypeptide or in the same molecular complex forming the channel itself. The extracellular binding of the ligand, either hormone or neurotransmitter, can trigger channel opening and thus Ca^{2+} entry.

ii. **G-protein-Operated Ca^{2+} channels:** the function of these channels is mediated by the action of G proteins. These proteins exert a fundamental role in several intracellular transduction pathways that are activated by seven transmembrane receptors. G proteins are heterotrimeric molecules composed of α, β and γ subunits. In the resting state, G proteins carry GDP bound in a pocket of their α subunit. Stimulation of seven transmembrane receptors leads to GDP release, a GTP molecule from the cytoplasm takes its place. The heterotrimeric G protein then dissociates into two parts, a cytosolic Gα-GTP and a membrane-bound G$\beta\gamma$ dimer. These subunits are the active forms of the G protein and are capable of signalling to specific membrane-associated effectors such enzymes and ion channels.

iii. **Second-messenger Operated Ca^{2+} channels:** these channels are activated by second messengers produced or released after the activation of seven transmembrane- or enzyme-coupled receptors. The most common second messengers are cAMP, cGMP, IP_3, DAG, arachidonic acid and Ca^{2+} itself.

iv. **Store-Operated Ca^{2+} channels:** these channels are responsible for a Ca^{2+} entry in response to ER Ca^{2+} depletion. The key molecules responsible for this Ca^{2+} entry have been identified only recently; they are named Orai1, 2 and 3; these channels are located in the plasma membrane (Freske et al., 2006; Zhang et al., 2006). Thanks to its EF-hand domain, an ER located protein, Stim1, can "sense" the [Ca^{2+}] into ER lumen; upon store depletion Stim1 changes its distribution from diffuse to clustered in "puncta" and interacts with plasma membrane Orai (Roos et al, 2005; Liou et al., 2005). This protein-protein interaction is believed to lead to opening of Orai and Ca^{2+} entry (Clapham 2007).

2.3 Pathways leading Ca^{2+} out of cells

During the course of a typical Ca^{2+} transient, the reaction that cause an increase in intracellular [Ca^{2+}]i ("on" reactions) are counteracted by the reactions that cause a decrease in [Ca^{2+}]i ("off" reactions); the "off" reactions depend on various pumps and exchangers that remove Ca^{2+} from cytosol (Fig. 2.1). These mechanisms assure that [Ca^{2+}]i at resting is maintained at ~100 nM and that internal stores are kept loaded. While sarco/endoplasmic reticulum Ca^{2+} ATPases (SERCA) pumps can accumulate Ca^{2+} in the ER lumen, there are two main mechanisms that extrude Ca^{2+} out off the cells, the plasma membrane Ca^{2+} ATPases (PMCA) and the Na^{+}/Ca^{2+} exchangers (NCX). The diverse PMCA, SERCA and NCX molecular toolkit, enables cells to select the combination of "off" reactions that exactly met their Ca^{2+}-signalling requirements (Berridge et al., 2003). The PMCA is an ubiquitous plasma membrane protein of ~ 125-140 KDa that catalyses the Ca^{2+} active transport out of the cell. The energy required for this reaction is supplied by ATP hydrolysis. The Ca^{2+}/ATP stoichiometry is 1/1. PMCA is classified as a type P pump since its mechanism of Ca^{2+} extrusion is mediated by the formation of a phosphorilated intermediate during the reaction cycle. PMCA has a lower transport rate compared to NCX, but a higher affinity, and thus it function as a housekeeping protein that controls [Ca^{2+}]c at resting state. Four different genes codifying for PMCA are present in higher eukaryotes; their expression pattern, the existence of splice variants and the regulation of PMCA activity by various mechanisms, in particular the binding of Ca^{2+}- CaM, are an explanation for its flexibility in responding to different tissue or cell-specific Ca^{2+} homeostasis demands (Carafoli 2005).

The NCX is an electrogenic antiport located in the plasma membrane; it exchanges three moles of Na^{+} for one mole of Ca^{2+}, either inward or outward, depending on the electrochemical gradients across the membrane. Thanks to its lower affinity for Ca^{2+}, but higher transport rate if compared to PMCA, it constitute the principal Ca^{2+} extrusion system in excitable cells.

A closely related family of exchangers, the Na^{+}/Ca^{2+}-K^{+} exchange (NCKX) gene family, has been recently discovered (Huang-Collet et al., 1999). This family of proteins comprises four members; NCKXs exchange four moles of Na^{+} for one mole of Ca^{2+} and one mole of K^{+} (Rizzuto and Pozzan, 2006).

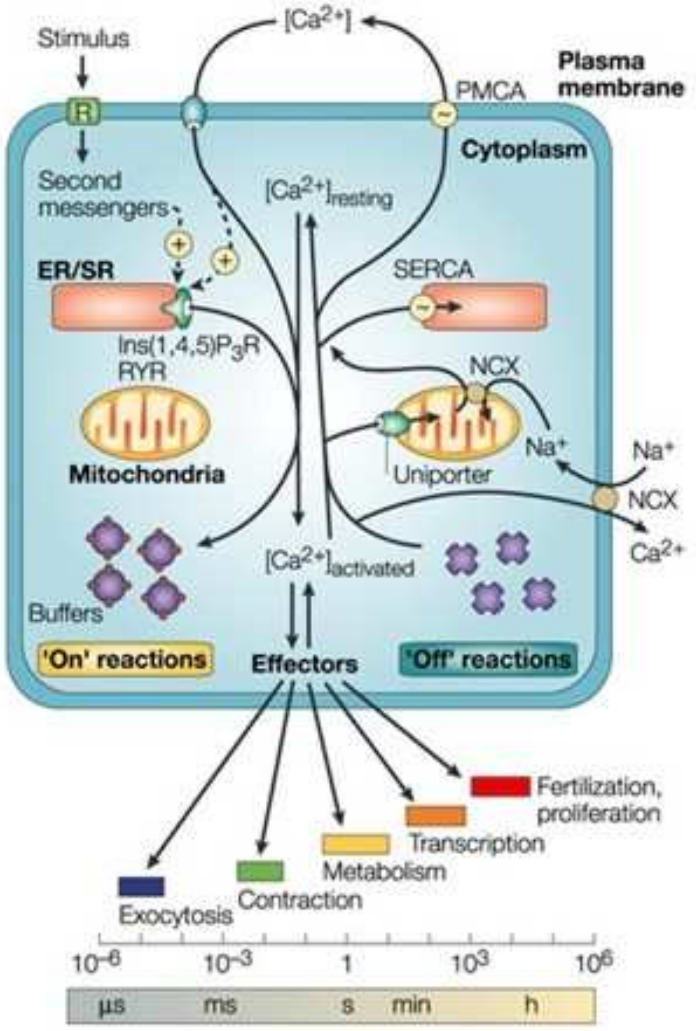

Figure 2.1. Calcium-signalling dynamics and homeostasis. During the "on" reactions, stimuli induce both the entry of external Ca^{2+} and the formation of second messengers that release internal Ca^{2+} that is stored within the ER/SR. Most of this Ca^{2+} (shown as red circles) is bound to buffers, whereas a small proportion binds to the effectors that activate various cellular processes that operate over a wide temporal spectrum. During the "off" reactions, Ca^{2+} leaves the effectors and buffers and is removed from the cell by various exchangers and pumps. NC(K)X and PMCA extrude Ca^{2+} to the outside, whereas SERCA pumps Ca^{2+} back into the ER. Mitochondria also have an active function during the recovery process in that they sequester Ca^{2+} rapidly through a uniporter, and this is then released more slowly back into the cytosol to be dealt with by the SERCA and the PMCA. Cell survival is dependent on Ca^{2+} homeostasis, whereby the Ca^{2+} fluxes during the "off" reactions exactly match those during the "on" reactions. [Ca^{2+}], Ca^{2+} concentration; Ins(1,4,5)P_3R, inositol-1,4,5-trisphosphate receptor; RYR, ryanodine receptor. Adapted from Berridge et al., 2003.

2.4 Intracellular Ca^{2+} stores

Several subcellular compartments exert a role in Ca^{2+} homeostasis by accumulating or releasing it and also by shaping its transients: mitochondria, Golgi apparatus, exocytotic vesicles and nuclei. However, the main Ca^{2+} store is the endoplasmic reticulum (ER) or sarcoplasmic reticulum (SR), its muscle equivalent (Pozzan et al., 1994, Rizzuto and Pozzan 2006).

2.4.1 The endoplasmic reticulum

In many cell types the increases in $[Ca^{2+}]c$ can be due, at least in part, to the release of Ca^{2+} from the ER (and to its specialization of muscle cells, the sarcoplasmic reticulum, SR). This compartment houses several proteins that actively regulate the traffic of molecules from and towards the ER (proteins, ions, etc.). Some of these proteins are involved in the fine control of its $[Ca^{2+}]$. Ca^{2+} accumulation by the ER depends on the SERCAs, transmembrane proteins that pump Ca^{2+} in the ER lumen with a 2:1 stoichiometry between Ca^{2+} ions and ATP. SERCA has the same membrane topology and mechanism of action of PMCA pump. There are several drugs that block SERCA pumps as the irreversible inhibitor thapsigargin (Tg), or the reversible ones cyclopiazonic acid (CPA) and 2,5-di-(ter-butyl)-1,4-benzohydroquinone (t-BHQ). The SERCA pump allows to reach a high $[Ca^{2+}]$ within the ER lumen, from ~ 200 μM up to 1 mM. Within the ER Ca^{2+} binds to Ca^{2+} buffering proteins, endowed with low-affinity (K_d about 1 mM), e.g. calreticulin. Bound and free Ca^{2+} is in very rapid equilibrium and the cation is readily released into cytosol when ER Ca^{2+} channels open. Ca^{2+} release from this organelle is therefore tightly controlled by several factors, including Ca^{2+} itself and an expanding group of messengers, such as inositol-1,4,5-trisphosphate (IP3), cyclic ADP ribose (cADP-R), nicotinic acid adenine dinucleotide phosphate (NAADP) and sphingosine-1-phosphate that either stimulate or modulate the Ca^{2+} release channels on the ER. Ca^{2+} is released from the ER by mainly two distinct channels, the IP3 receptor (IP3-R) and the ryanodine receptor, found primarily, but not exclusively, in excitable cells. IP3 is a second messenger whose cytosolic production is triggered by agonist binding to G- coupled protein receptors that in turn activate pospholipase C. The most important modulator of the IP3-Rs is Ca^{2+} itself. IP3 binding increases the Ca^{2+} sensitivity of the receptor that shows a biphasic modulation since it is activated at low $[Ca^{2+}]c$ (250-300 nM), but is blocked at higher micromolar concentrations that occur upon Ca^{2+} release. In addition to these cytosolic actions,

Ca^{2+} can also sensitise the IP3-Rs by functioning from the ER lumen. The IP3-Rs activity can also be modulated through the phosphorylation by different protein kinases such as protein kinase A (PKA), protein kinase C (PKC) or Ca^{2+}-calmodulin dependent protein kinases (Da Silva et al., 2000). To date, three IP3Rs subtypes have been identified, that differ both in tissue and levels expression or affinity for IP3 (Carafoli 2005).

2.4.2 The Golgi apparatus

Golgi apparatus came to the scene of cellular Ca^{2+} homeostasis only recently, thanks to an engineered form of Aequorin (a Ca^{2+}-sensitive photoprotein) that includes a target sequence for this organelle. It has been seen that Golgi apparatus not only can accumulate Ca^{2+} within its lumen, but also actively participates in cellular Ca^{2+} signalling (Pinton et al., 1998). Golgi apparatus appears to contain SERCA- type pumps but also a Ca^{2+}-ATPase named secretory pathway Ca^{2+}-ATPase (SPCA). Golgi releases Ca^{2+} upon cellular stimulation with IP3-production coupled agonists through an IP3-modulated channel (Carafoli 2005).

2.4.3 Mitochondria

That mitochondria play a role in Ca^{2+} homeostasis has been known for over 40 years. These organelles, in fact, can accumulate Ca^{2+} in their matrix by action of a uniporter that transports Ca^{2+} at the expense of the membrane potential, $\Delta\Psi$, negative inside, across the inner mitochondrial membrane ($\Delta\Psi$ ~ -180 mV) generated by the respiratory chain. Ca^{2+} never reaches electrochemical equilibrium with the membrane potential because in the inner membrane there are proteins that act as antiports that extrude Ca^{2+} from the matrix in exchange with H^+ or Na^+. The identification of the kinetic properties of these transporters, and of the uniport in particular, led many investigators to conclude that mitochondria play little role in physiological Ca^{2+} homeostasis. In fact their affinity was found to be too low to significantly accumulate the cation not only in resting conditions, but also during the transient $[Ca^{2+}]c$ increases generated by cell stimulation (Pozzan et al., 2000). However, using selectively mitochondria targeted aequorin it was demonstrated that agonist-evoked transient $[Ca^{2+}]c$ increase results in rapid and massive Ca^{2+} increase that reaches values 10-50-fold higher than in the cytosol (Rizzuto et al, 1992; Rizzuto et al.,1998). This unexpected finding was explained by the so called “microdomain hypothesis”. The idea is that mitochondria are located in microdomains where, upon Ca^{2+} mobilization from the ER, local $[Ca^{2+}]$ can reach very high levels, for example in proximity of IP3-sensitive channels (Rizzuto

et al., 1993). Subsequently direct evidence for close interactions between mitochondria and ER have been provided (Rizzuto et al., 1998), and recent works have demonstrated that these interactions are stable in time (Filippin et al., 2003). Recent work by De Brito and Scorrano (DeBrito and Scorrano, 2008) has demonstrated that such close interactions depend on the omotypic interaction of mitofusin 2, expressed on the ER and outer mitochondrial membrane.

Ca^{2+} entry into mitochondrial matrix exerts different physiological functions ranging from activation of three mitochondrial dehydrogenases (the pyruvate, α- keto-glutarate and isocitrate dehydrogenase), thus positively regulate ATP synthesis, to buffering and modulation of cytosolic Ca^{2+} variations (Giacomello et al., 2007).

3. Ca^{2+} SENSORS

The study of cellular Ca^{2+} homeostasis in physiological and pathological conditions requires methods to accurately monitor the dynamics of $[Ca^{2+}]$ in living cells. It is not surprising that advancements in the understanding of Ca^{2+} signalling were thus strictly linked to advancements in Ca^{2+} probes performances. These molecules are characterized by the capacity to bind Ca^{2+} selectively and reversibly, and this event cause a physicochemical change in the probe that renders easy to distinguish between its free and Ca^{2+}-bound form. In the vast majority of Ca^{2+} probes, changing in the absorbance and / or emission of light are used, even if other probe's features, like nuclear magnetic spectrum, have been also used in a few cases. Although this is obvious to specialists, it should be mentioned that every Ca^{2+} sensor measures the $[Ca^{2+}]$ indirectly; what is actually measured is in fact the concentration of the free *vs* complexed probe (based on the physicochemical changes aforementioned) and the effective $[Ca^{2+}]$ can then be calculated from these values and the probe dissociation constant (k_d) (Rudolf et al., 2003).

A first classification of Ca^{2+} probes distinguishes between ratiometric and non ratiometric probes (Fig. 3.1).

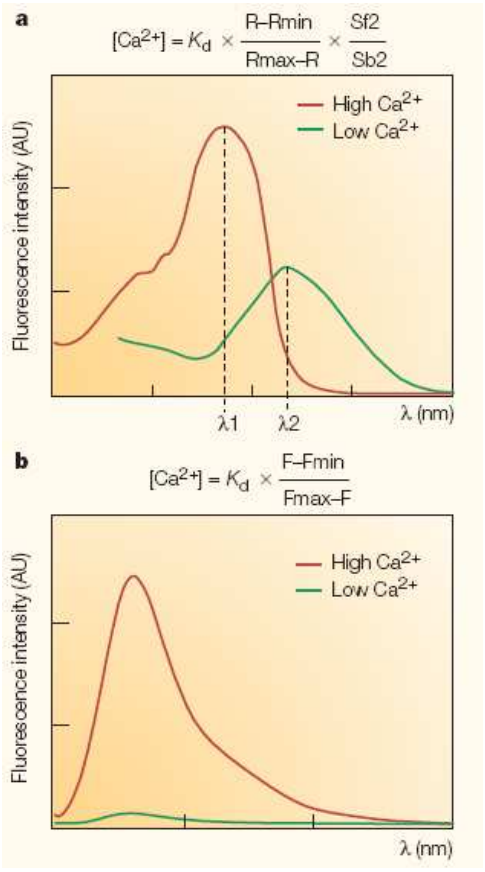

Figure 3.1. Excitation and emission spectra of ratiometric and non-ratiometric Ca^{2+} probes. a. Ratiometric Ca^{2+} probes have excitation/emission spectra that change upon Ca^{2+} binding. $[Ca^{2+}]$ is obtained by a ratio between the fluorescence intensity of the bound and unbound form., λ1 and λ2. b. Non-ratiometric Ca^{2+} probes change their fluorescence intensity (F) upon Ca^{2+} binding. Adapted from Rudolf et al., 2003.

Ratiometric probes (Fig. 3.1, a) are characterized by an excitation (or emission) spectrum that changes upon Ca^{2+} binding; Ca^{2+} concentration can be measured as a ratio between a fluorescence intensity value taken at two wavelength (λ), λ1 for the bound form and λ2 for the free one. This ratio corrects for unequal dye loading, probe's compartimentalization, focal plane shift and bleaching. These advantages are counteracted by the complexity of the instrumentation required for exciting/acquiring the signal at two different wavelengths.

Non ratiometric dyes (Fig. 3.1, b), on the contrary, increase their fluorescence proprieties upon Ca^{2+} binding; Ca^{2+} concentration is easy to detect, since a single excitation/ acquisition system is required, but there is no possibility of correction for focal plane shift, unequal dye loading, etc…. Moreover, to obtain absolute [Ca^{2+}] values a calibration is required; this is usually not trivial to perform.

A second classification of Ca^{2+} sensors is between synthetic and genetically encoded indicators, as explained below.

3.1 Synthetic Ca^{2+} indicators

The first rationally-designed fluorescent Ca^{2+} indicator (quin2) was synthesized by Roger Tsien and derives from the well-known specific Ca^{2+} chelator EGTA (Tsien, 1980). The substitution of two methylene groups with two benzene rings couples the conformational change due to Ca^{2+} binding to a change in the spectral proprieties of the dye. Improvements of the original polycarboxilate indicators were then achieve in the following years (all in R.Y Tsien laboratory), e.g. the synthesis of indicators with different Ca^{2+} affinities and with excitation wavelengths different from the ultraviolet one (characteristic of the first generation of indicators). The most popular modification of these dyes, that has rendered their use very easy, was the synthesis of their hydrophobic acetoxymethil (AM) ester forms. While the original dyes have to be microinjected into cells by a time-consuming technique, AM esters can simply be added to the medium; due to their hydrophobicity, the AM esters of the dyes simply diffuse across the plasma membrane and then they are hydrolized by cellular esterases, thus freeing the hydrophilic, original dye, that can not longer leave the cytoplasm.

The simplicity of dye loading and Ca^{2+} measurement setup, with the huge signal differences between bound and free form of the probe have led to a large use of these Ca^{2+} indicators. The main disadvantage is the difficulty to target them into subcellular compartments: although a mitochondrial synthetic dye has been produced (rhod-2) (Minta et al., 1989), which accumulates into mitochondrial matrix thanks to its positive charge (and others techniques have been proposed in order to target a synthetic dye preferentially into a

subcellular compartment, (Csordas et al., 1999)), the results are far from ideal, and to this end usually genetically encoded Ca^{2+} probes are preferred.

3.2 Genetically encoded Ca^{2+} indicators

The second family of Ca^{2+} indicators comprises proteins, either chemiluminescent (Aequorin) or Green Fluorescent Protein (GFP)-based, both derived from the medusa *Aequorea Victoria*. Their main advantage is the possibility to modify, by simple molecular biology techniques, their coding sequences in order to target them into a specific subcellular localization or to obtain different Ca^{2+} affinities and tuneable spectroscopic features. On the other hand, the main disadvantage is the need of a cDNA transfection that in some cell types, especially primary cultures, may have a low efficiency. However, due to new transfection techniques, e.g., electroporation with mild condition, virus infection and the possibility to generate stable clones and even transgenic animals that express the Ca^{2+} probes, this disadvantage is of lower importance if compared to few years ago.

3.2.1 Aequorin

Aequorin is a 21- KDa chemiluminescent protein originally purified from the medusa *Aequorea Victoria*, where, in association with GFP, is responsible for jellyfish bioluminescence (Shimomura et al., 1962). Aequorin application was greatly enhanced thanks to the cloning of its cDNA in 1985 by Prasher et al. (Prasher et al., 1985); after this, both its subcellular localization and Ca^{2+} affinity have been modified in order to measure [Ca^{2+}] not only in the cytosol, but also in organelles such as mithochondria, ER, Golgi apparatus and nucleus. Aequorin is endowed with three EF-hand domains that bind Ca^{2+}; upon Ca^{2+} binding the apoprotein, that is associated with its coenzyme coelenterazine, emits a photon while peroxidation of the coenzyme to coelenteramide “burns” the enzyme that is no longer able to emit blue light upon Ca^{2+} binding. The main disadvantages of this system are: i) the need of a cofactor that has to be externally supplied; ii) the intrinsic low signal emitted by Aequorin upon Ca^{2+} binding that largely prevents its use in single cell measurements.

3.2.2 GFP-based probes

Thanks to its unique features among fluorescent probes, GFP has tens of application in cell biology. Its first advantage is that it doesn't require an external cofactor in order to emit light: its chromophore is obtained from its amino acids 65 to 67 by a mechanism of cyclization, dehydration and oxidation. Moreover, this chromophore is located into an α-helix running inside a tight structure formed by an 11-stranded β-barrel, and so is protected against environmental condition's variations, at least in the wild-type form (Tsien, 1998). GFP fluorescence is unaffected by different modification: e.g, an insertion of different protein in position 145, and even also circular permutation, in which GFP is spliced in two parts and then the amino and carboxyl-termini are interchanged. These modifications, however, allow GFP fluorescence to be perturbed by conformational changes of proteins that are inserted at the amino, carboxyl-termini or inside GFP, thus rendering GFP able to indirectly measure different subcellular parameters, like pH or second messengers concentration. Different GFP mutants have been also generated that bear mutations in the amino acids responsible for chromophore formation or located in its proximity, thus shifting fluorescence emission from blue to yellow, obtaining more brighter variants or mutants with decrease environmental sensitivity. The most utilized GFP variants are:

i. **GFP (S65T) or eGFP**: wild-type GFP has two excitation peaks, a major (395 nm) and a minor one (475nm). In this GFP mutant, the substitution of a Ser with an aliphatic residue causes a suppression of the 395 nm peak and a five to six fold enhancement of the higher wavelength peak, whose maximum excitation is now at 490 nm instead of 475 nm.

ii. **Blue fluorescent protein (BFP or GFP(Y66H/Y145F)) :** this mutant emits blue light when excited with UV light; however, due to the potential toxicity of UV light for biological samples and its low quantum yield this mutant was substituted for many application with CFP.

iii. **Cyan fluorescent protein (CFP or GFP(Y66W)) :** this mutant has excitation and emission spectra intermediate to those of BFP and EGFP.

iv. **Yellow fluorescent protein (YFP or GFP(T203Y))** : this mutant, and its ameliorations, is one of the most widely used GFP mutants and has a red-shifted spectrum. YFPs, due to changes in internal hydrogen bonding and steric packaging, are the more sensitive to photobleaching, decolorization by protonation and quenching by many anions, of which chloride is the most

physiologically relevant. While these features can be desiderable in order to measure pH variations, for others application they may constitute a problem, and so many mutant were analyzed in order to lower this environmental sensitivity. The most widely used are citrine (Griesbeck et al., 2001), and Venus (Nagai et al., 2002). Citrine carries a series of mutation, the most important being Q69M, that improve folding at 37°C and lowers chloride and proton sensitivity, since its pKa is 5.7. Venus is characterized by a pKa of 6 and a very fast maturation *in vivo*. Moreover circular permutation of YFPs further improves their spectroscopic features.

v. **Many more GFPs**, derived from species other than Aequorea Victoria, have been produced over the last few years and a whole palette of fluorescent properties is presently available. The interested reader is referred to the reviews by Shaner et al. or Miyawaki for further details (Shaner et al., 2001; Miyawaki 2005). Given that in my thesis I have used only CFP and YFP (and their variants) I will not further discuss this point.

3.2.2.1 Single GFP Ca^{2+} probes: Camgaroo and Pericam

Both Camgaroo and Pericam Ca^{2+} probes are based on a EYFP whose chromophore and surrounding hydrogen network are sensitive to probe conformational variations. In this Ca^{2+} probe, named Camgaroo (Fig. 3.2, b), a EYFP is splitted in two parts and the aforementioned residue 145, the GFP amino acid that admits peptide insertions without loose of GFP fluorescence, was substituted by *Xenopus* CaM, that functions as Ca^{2+} sensor (Baird et al., 1999). In Pericams (Nagai et al., 2001) a EYFP was circularly permuted and its carboxy-terminus was fused to CaM, while its amino-terminus was fused to M13, a 26 AA-peptide derived from the CaM-binding peptide of the skeletal muscle myosin light chain kinase. Upon Ca^{2+} binding, M13 peptide wraps around CaM and this cause a conformational change that in turn produces a fluorescence variation of EYFP (Fig. 3.2, c).Three different pericams were generated: i) flash pericam, that becomes brighter upon Ca^{2+} binding; ii) inverse pericam, that on the contrary decreases its fluorescence upon Ca^{2+} binding and iii) ratiometric pericam, endowed with an excitation wavelength changing in a Ca^{2+} -dependent manner, thus allowing a ratiometric Ca^{2+} measurement. The main drawback of this class of Ca^{2+} sensor is its pH sensitivity, and, with the exception of ratiometric pericam, the fact that only a fluorescence intensity change is measured.

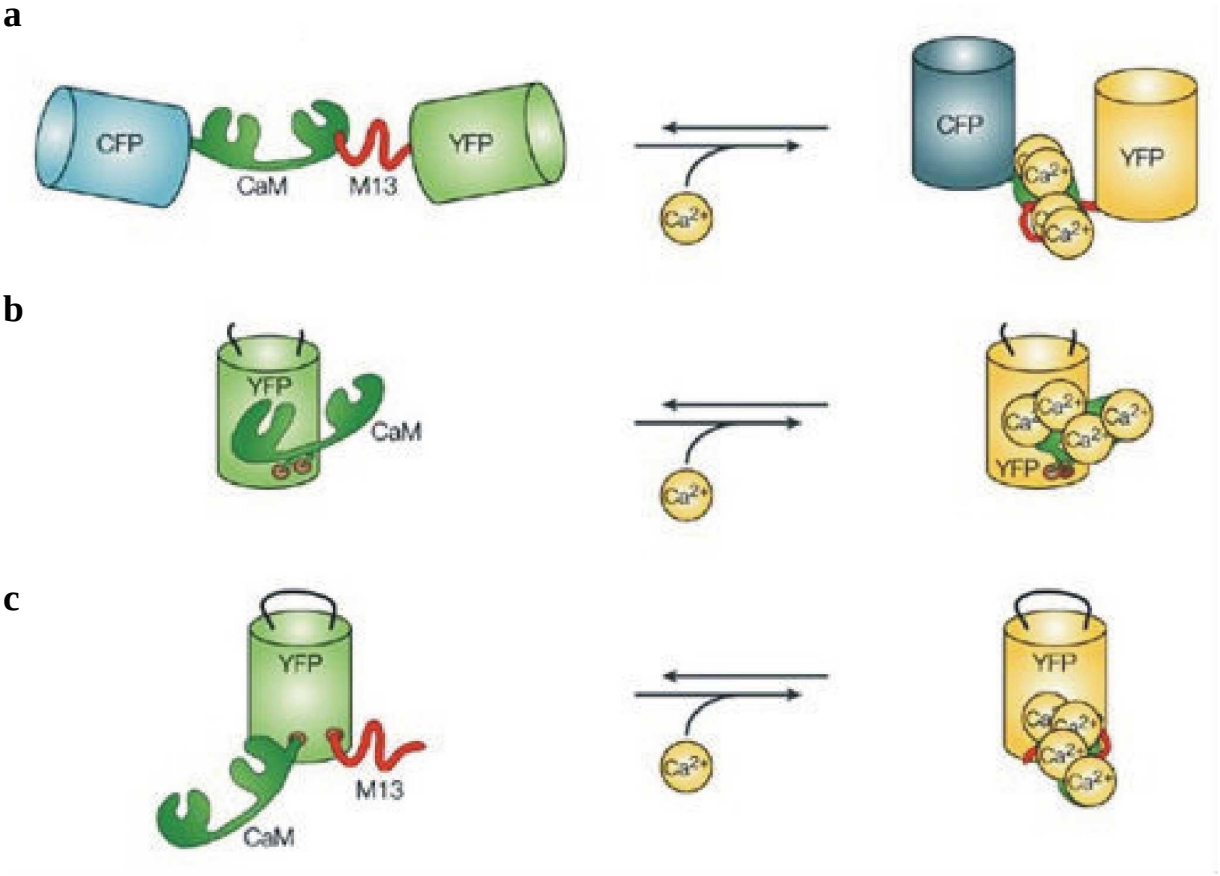

Figure 3.2. Calcium probes based on GFP mutants. a. Cameleon: upon Ca^{2+} binding, there is a conformational change that in turn causes an increase in FRET. b. Camgaroo: CaM is inserted in a YFP, Ca^{2+} binding cause an increase in fluorescence. c. (Ratiometric) Pericam: CaM and its binding peptide are cloned at the amino and carboxyl-termini of a circularly permuted YFP. Upon Ca^{2+} binding a change in the surrounding environment of the chromophore causes a shift in the spectral proprieties of the probe. See text for details. Adapted from Rudolf et al., 2003.

3.2.2.2 Two-GFP Ca^{2+} probes: Cameleons

Cameleon probes are made up of two GFP mutants linked by CaM and M13 peptide (Fig. 3.2, a). The couple of mutants can be BFP- GFP or, most commonly, CFP-YFP: the general requirement is that the excitation spectrum of the acceptor moiety (GFP or YFP) partially overlaps the emission spectrum of the donor moiety (that is, BFP or CFP) (Fig. 3.3). Cameleon probes (Miyawaki et al., 1997) are based on the phenomenon of Fluorescence (or Föster) Resonance Energy Transfer (FRET); a phenomenon that occurs when two fluorophores are in sufficient proximity (that is 1-10 nm) and at an appropriate relative orientation such that the excited fluorophore (donor) can transfer its energy to a second,

longer wavelength fluorophore (acceptor) in a non-radiative manner. Thus, only if the two GFP mutants are in close proximity and with an appropriate orientation, excitation of the donor causes an emission at the typical wavelength of the acceptor. In cameleons, CaM and M13 peptide constitute the molecular switch that allows the probe to couple Ca^{2+} variations to FRET variations. When CaM is not bind to Ca^{2+}, the probe is in an "open" conformation (Fig. 3.3, a); the distance between the donor and the acceptor is too high for FRET to occur. In this condition, donor excitation (e.g, 440 nm in the case of CFP) causes an emission at its own wavelength (that peaks at 480 nm).

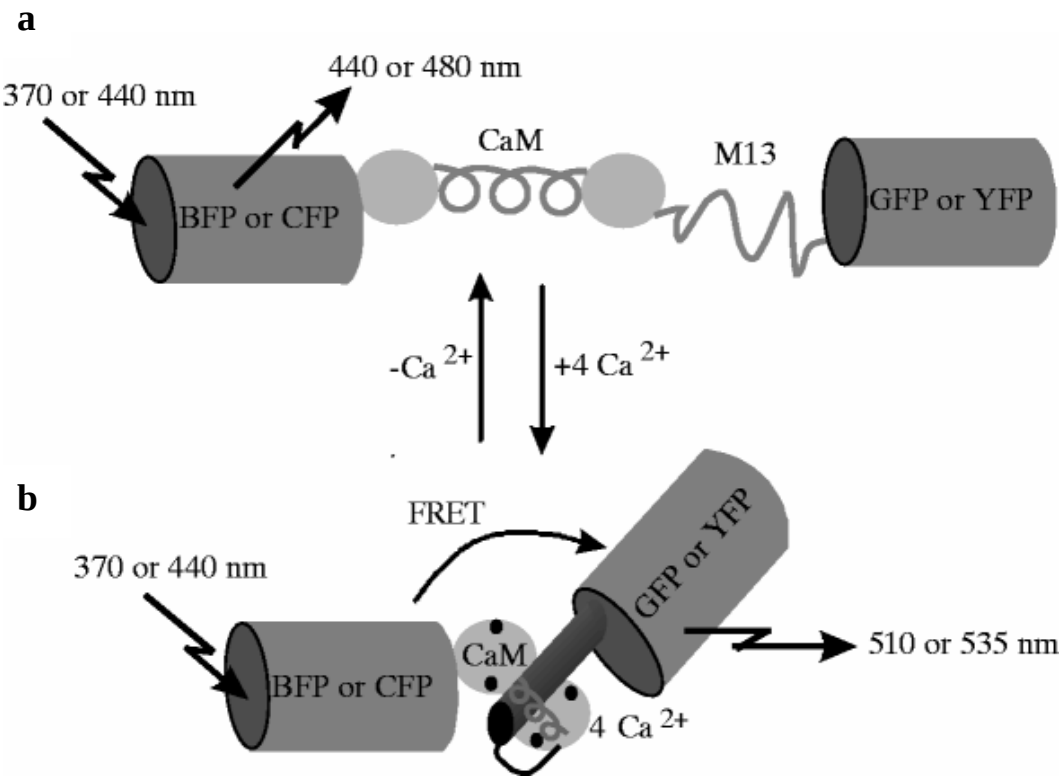

Figure 3.3. Schematic structure of cameleon probe and of its functioning. a. At low [Ca^{2+}], excitation of the donor (BFP or CFP) cause an emission at its typical wavelength. b. Upon Ca^{2+} binding to CaM, M13 wraps around CaM and this cause a conformational change, allowing FRET between donor and acceptor (GFP or YFP) to occur. This causes a rise in acceptor emission and a drop in donor emission. The ratio of these two values is proportional to [Ca^{2+}]. Adapted from Miyawaki et al., 1997.

When there is a Ca^{2+} rise, the ion binds to CaM; consequently, M13 wraps around CaM causing a conformational change of the whole cameleon protein: in this "close" conformation, donor and acceptor are in close proximity and there is a rise in FRET (Fig. 3.3,

b). In this case, donor excitation at 440 nm causes only a minor emission at 480 nm, the vast majority of its energy is transferred to the donor that in turn emits at a longer wavelength, that peaks at 535 nm in the case of YFP. So, the ratio between acceptor and donor emission upon donor excitation is proportional to [Ca^{2+}].

Cameleons possess all the advantages of genetically coded Ca^{2+} probes: indeed, in few years cameleons targeted to different subcellular compartments and with different Ca^{2+} affinities were developed. Moreover, cameleons are ratiometric probes. As for camgaroos and pericams, the YFP moiety was ameliorated in order to lower its pH sensitivity and so cameleons with citrine or Venus as acceptor, either normal or circularly permutated, were produced (Miyawaki et al., 1999).

Cameleons still suffer of a problem that became soon evident when it was employed to measure subcellular Ca^{2+} dynamics under the plasma membrane: it failed to respond properly, probably because of an excess of endogenous CaM interacting with cameleon M13 peptide. To solve this problem, Palmer et al. reengineered CaM and M13 amino acids sequences and obtained four cameleons with different Ca^{2+} affinities and that are no longer sensitive to endogenous calmodulin. These new cameleons endowed with citrine as acceptor are named D1, D2, D3 and D4, while those that possess Venus as acceptor are named D1cpv, D2cpv, D3cpv and D4cpv (Palmer et al., 2006) (Fig. 3.4).

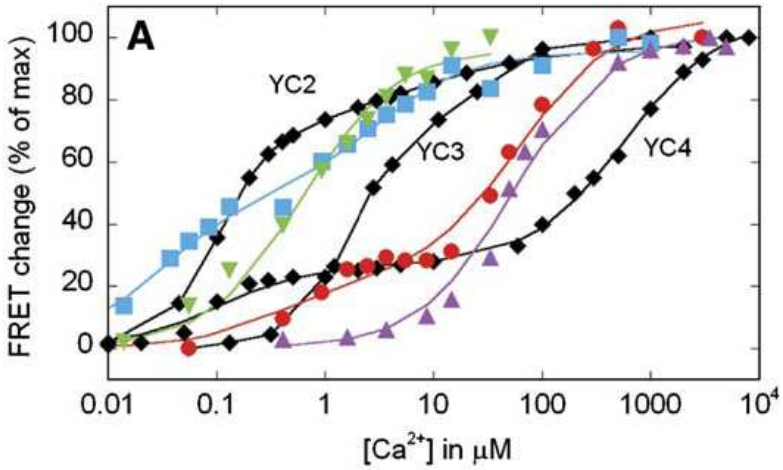

Figure 3.4 In vitro calibration of the newly designed cameleons. Ca^{2+} tritation curves of the new redesigned and original camelons probes. Blue: D2cpv, Green: D3cpv, Red: D1, Purple: D4cpv. The black lines are referred to the original constructs with the same Ca^{2+} affinity (YC 2, 3 and 4). Adapted from Palmer et al., 2006.

4. AIM AND SIGNIFICANCE OF THIS WORK

Ca^{2+} signalling exerts a plethora of functions in cells and its regulation both in physiological and pathological conditions is widely studied. In these last years, the role of subcellular compartments like ER, mitochondria, nucleus and Golgi apparatus in Ca^{2+} handling has been largely unravelled thanks to the generation of genetically encoded Ca^{2+} probes. It is thus surprising that the possible role of peroxisomes in cellular Ca^{2+} homeostasis has never been investigated (until very recently). One may indeed speculate that a fundamental second messenger like Ca^{2+} should also modulate some of the enzymatic activity housed within peroxisomal matrix, or/and that peroxisomes can constitute an additional cellular Ca^{2+} buffer organelle, but this can and need to be investigated directly.

The first part of this study was thus aimed to investigate if peroxisomes take part to cellular Ca^{2+} handling and, if yes, to characterize the basic features and the pharmacological sensitivity of this phenomenon. Cameleons were chosen as Ca^{2+} sensors for this study since they allow a ratiometric (and thus easily calibrated) Ca^{2+} measurements at the single cell (and organelle) level. Cameleons were targeted into peroxisomal matrix and the experiments described below demonstrate that peroxisomes are in equilibrium with cytosolic Ca^{2+} and they experience slow $[Ca^{2+}]$ rises upon cellular stimulation. This phenomenon seems to be driven by the Ca^{2+} gradient itself and thus peroxisome appears to represent another Ca^{2+} buffering organelle.

This first demonstration can constitute the basis for following studies aimed at understanding if, and how, Ca^{2+} and its variations can regulate peroxisomal functions. One example will be discussed in the second part of this work, where experiments supporting an *in vivo* Ca^{2+} regulation of a peroxisomal plant H_2O_2 scavenging enzyme are provided.

RESULTS AND DISCUSSION

5.1 Calcium dynamics in the peroxisomal lumen of living cells (published paper)

THE JOURNAL OF BIOLOGICAL CHEMISTRY VOL. 283, NO. 21, pp. 14384–14390, May 23, 2008

Calcium Dynamics in the Peroxisomal Lumen of Living Cells*[S]

Received for publication, January 23, 2008, and in revised form, March 20, 2008 Published, JBC Papers in Press, March 24, 2008, DOI 10.1074/jbc.M800600200

Ilaria Drago[‡], Marta Giacomello[‡], Paola Pizzo[‡], and Tullio Pozzan[‡§1]

From the [‡]Department of Biomedical Sciences and Consiglio Nazionale delle Ricerche Institute of Neuroscience, University of Padua and [§]Venetian Institute of Molecular Medicine, 35121 Padua, Italy

We here describe the generation of novel, green fluorescent protein-based Ca^{2+} indicators targeted to the peroxisome lumen. We show that (i) the Ca^{2+} concentration of peroxisomes in living cells at rest is similar to that of the cytosol; (ii) increases in cytosolic Ca^{2+} concentration (elicited by either Ca^{2+} mobilization from stores or Ca^{2+} influx through plasma membrane Ca^{2+} channels) are followed by a slow rise in intraperoxisomal $[Ca^{2+}]$; (iii) Ca^{2+} influx into peroxisomes is driven neither by an ATP-dependent pump nor by membrane potential nor by a $H^+(Na^+)$ gradient. The peroxisomal membrane appears to play a low pass filter role, preventing the organelle from taking up shortlasting cytosolic Ca^{2+} transients but allowing equilibration of the peroxisomal luminal $[Ca^{2+}]$ with that of the cytosol during prolonged Ca^{2+} increases. Thus, peroxisomes appear to be an additional cytosolic Ca^{2+} buffer, but their influx and efflux mechanisms are unlike those of any other cellular organelle.

A variation in cytosolic Ca^{2+} is a key component of the cell signaling machinery activated by receptor stimulation. Although a plethora of information is available regarding Ca^{2+} dynamics in different subcellular compartments, a notable exception is represented by peroxisomes, single membrane-bound organelles diffusely distributed within the cytosol of virtually all eukaryotic cells (1). Proteins located in the peroxisomal matrix are linked to different biochemical pathways (2) such as the β-oxidation of fatty acids and detoxification of hydrogen peroxide. The latter pathway is exclusively localized in the peroxisomal compartment of fungi and plants, whereas in mammalian cells it is distributed between peroxisomes and mitochondria (2). Specialized peroxisomal functions, such as fatty acid degradation and synthesis of phytohormones, are found in some cells, (*e.g.* plants and fungi) (3). Interest in peroxisomes has increased recently due to the discovery that defects in peroxisomal biogenesis and peroxisomal enzyme deficiencies are linked to several genetic disorders in humans (4). Given that any enzymatic activity is highly sensitive to the ionic composition of the surrounding environment, it is surprising that information on the luminal ion content of peroxisomes is scarce and contradictory. In particular, no data are currently available on Ca^{2+} concentration in the peroxisome lumen, $[Ca^{2+}]_P$.

We here present a novel probe, derived from the new green fluorescent protein (GFP)[2]-based Ca^{2+} indicators (Dcpv) (5), for monitoring $[Ca^{2+}]_P$ in living cells. We show that peroxisomes contribute to the sequestration of part of the Ca^{2+} entering the cytoplasm during cell activation in a way that is unique among cellular organelles.

MATERIALS AND METHODS

Constructs—The sequence coding for the tripeptide SKL was introduced before the stop codon of D3cpv (kindly provided by R. Tsien, San Diego, CA) by PCR using the oligonucleotides 5′-ACCCAAGCTTGCCACCATG-3′ (forward); 5′-ACCCAAGCTTGCCACCATG-3′ (reverse). The resulting PCR product was digested with HindIII and EcoRI and ligated into pcDNA3 (Invitrogen). PCR for introducing the KVK coding sequence was performed using D3cpv-SKL as a template with the same forward primer and the following reverse: 5′-ACCCAAGCTTGCCACCATG-3′. The cDNA of pHluorin was a kind gift from S. Grinstein (Toronto, Canada).

Cell Culture and Transfection—HeLa cells were grown in Dulbecco's modified Eagle's medium containing 10% fetal calf serum supplemented with L-glutamine (2 mM), penicillin (100 units/ml), and streptomycin (100 μg/ml) in a humidified atmosphere containing 5% CO_2, while GH3 cells were grown in the same medium supplemented with non-essential amino acid (Sigma). Cells were seeded onto glass coverslips (24-mm diameter); for GH3 cells, coverslips were pretreated with poly-L-lysine (50 μg/ml). Transfections were performed at 60% confluence using TransIT®-LT1 transfection reagent (Mirus, Bologna, Italy) with 1 μg of DNA. Fluorescence experiments were performed 48 h after transfection.

Cell Loading with Fura-2, BCECF, or BAPTA—To monitor cytosolic $[Ca^{2+}]$ or pH, cells seeded on coverslips were incubated with 1 μM fura-2/AM or 2 μM BCECF/AM in an extracellular-like solution for 30 min at 37 °C, washed, and then incubated for 30 min at room temperature. In the experiments aimed at reducing cytosolic and organelle $[Ca^{2+}]$ to the lowest possible level, cells were loaded contemporaneously with 1 μM fura-2/AM and 10 μM BAPTA/AM using the protocol described above in a medium without $CaCl_2$ and supplemented with 500 μM EGTA.

* This work was supported in part by grants from Italian Telethon, AIRC (Italian Association for Cancer Research), the Cariparo Foundation (to T. P.), the University of Padua, and the Italian Ministry of University (FIRB 2004) (to P. P.). The costs of publication of this article were defrayed in part by the payment of page charges. This article must therefore be hereby marked "*advertisement*" in accordance with 18 U.S.C. Section 1734 solely to indicate this fact.

[S] The on-line version of this article (available at http://www.jbc.org) contains supplemental Fig. S1 and supplemental references and data.

[1] To whom correspondence should be addressed: Dept. of Biomedical Sciences, CNR Inst. of Neurosciences, University of Padua, Viale G Colombo 3, 35121 Padua, Italy. Tel.: 39-049-827-6067; Fax: 39-049-827-6049; E-mail: tullio.pozzan@unipd.it.

[2] The abbreviations used are: GFP, green fluorescent protein; TRH, thyrotropin-releasing hormone; BCECF, 2′,7′-bis-(2-carboxyethyl)-5-(and-6)-carboxyfluorescein; BAPTA, 1,2-bis(o-aminophenoxy)ethane-*N*,*N*,*N*′,*N*′-tetraacetic acid.

Cell Imaging—Cells expressing (or loaded with) the fluorescent probes were analyzed using an inverted fluorescence microscope (Zeiss Axioplan) with an immersion oil objective (×63, N.A. 1.40, for fluorescent probes and ×40, N.A. 1.3, for fura-2 and BCECF). Excitation light was produced by a monochromator (Polychrome II; TILL Photonics, Martinsried, Germany): 400 and 480 nm for pHluorin; 340 and 380 nm for fura-2; 495 and 440 nm for BCECF. The two excitation wavelengths were rapidly alternated and the emitted light deflected by dichroic mirrors (HQ 520 LP for pHluorin and BCECF and 455DRPL for fura-2) was collected through emission filters (HQ 520 LP for pHluorin and BCECF and 480 ELFP for fura-2). For the D3-derived probe, the excitation light was 425 nm. The emitted light was collected through a beamsplitter (OES s.r.l., Padua, Italy) (emission filters HQ 480/40M for cyan fluorescent protein and HQ 535/30 M for yellow fluorescent protein) and a dichroic mirror (515 DCXR). Filters and dichroic mirrors were purchased from Omega Optical and Chroma. Images were acquired using a cooled CCD camera (Imago; TILL Photonics) attached to a 12-bit frame grabber. Synchronization of the monochromator and CCD camera was performed through a control unit run by TILLvisION v.4.0 (TILL Photonics); this software was also used for image analysis. For time course experiments, the fluorescence intensity was determined over regions of interests covering small groups of peroxisomes or cytosolic regions (devoid of identifiable structures). Exposure time and frequency of image capture varied from 30 to 500 ms and from 5 to 0.2 Hz, respectively. Cells were mounted into an open-topped chamber thermostated at 37 °C and maintained in an extracellular medium containing (in mM): 135 NaCl, 5 KCl, 1 $MgSO_4$, 0.4 KH_2PO_4, 10 glucose, 20 Hepes, pH 7.4, at 37 °C. Plasma membrane permeabilization was performed by treating cells for 1 min with 100 μM digitonin in an intracellular-like medium containing (in mM): 130 potassium-gluconate, 10 NaCl, 1 KH_2PO_4, 1 $MgSO_4$, 20 Hepes, pH 7.0, at 37 °C and 500 μM EGTA. Experiments with permeabilized cells were performed in the same medium; where indicated, the latter was supplemented with a buffer containing (in mM): 2 EGTA, 1 H-EDTA, 1 $MgCl_2$, and variable $CaCl_2$ concentration.

Immunocytochemistry—Cells were fixed in phosphate-buffered saline containing 4% paraformaldehyde for 20 min, permeabilized with 0.1% Triton X-100 in phosphate-buffered saline containing 0.5% bovine serum albumin and 0.15% glycine (PBG) for 20 min, and blocked with 5% non-immune goat serum in PBG for 30 min. Rabbit anti-catalase (Rockland Immunochemicals, Gilbertsville, PA) or rabbit anti-PMP70 (Sigma) antibodies were added for 1 h at 37 °C. Samples were washed three times in PBG and then treated with Alexa Fluor 568 goat anti-rabbit IgG (Invitrogen) for 1 h at room temperature. Samples were washed three times in PBG and three times in phosphate-buffered saline, mounted with Mowiol (Sigma), and analyzed with a Leica TCS SP5 confocal microscope using an immersion oil objective (×63, N.A. 1.40). Image acquisition was performed by sequential scanning with excitation wavelengths of 488 nm for D3cpv-(KVK)-SKL and 543 nm for Alexa Fluor 568. Emission wavelengths were collected in the 495 to 535-nm (D3cpv-(KVK)-SKL) and 580 to 630-nm (Alexa Fluor 568) ranges. Correction of the bleed-through from the green fluorescence into the Alexa Fluor 568 channel and merging of the emitted fluorescence were carried out using the Acousto Optical Beam Splitter technique and the software provided by the manufacturer of the confocal microscope.

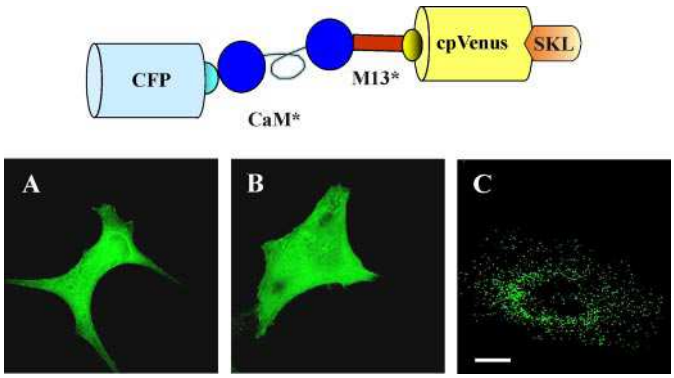

FIGURE 1. **Subcellular distribution of transiently expressed D3cpv-SKL in HeLa cells.** D3cpv, a new generation member of the Cameleon, fluorescence resonance energy transfer-based Ca^{2+} sensor family, carrying new mutations (*) in the Calmodulin (*CaM*) and M13 sequences (5), was modified by insertion at the C terminus of the peroxisome targeting signal SKL (*upper panel*). HeLa cells transiently expressing the new protein (*A*) or the original cytosolic probe (*B*) showed no difference in their subcellular distribution. Upon plasma membrane permeabilization with 100 μM digitonin (which results in complete release of the cytosolic probe), punctate structures scattered throughout the cytoplasm, later verified to be peroxisomes (see "Results" for details), became visible (*C*).

Materials—Cyclo piazonic acid, digitonin, carbonyl cyanide-4-(trifluoromethoxy)-phenylhydrazone, histamine, monensin, and thyrotropin-releasing hormone (TRH) were purchased from Sigma-Aldrich, ionomycin from Calbiochem, and fura-2/AM, BCECF/AM, and BAPTA/AM from Molecular Probes. All other materials were analytical or highest available grade.

Statistical Analysis—All the data are representative of at least five different experiments. Values are expressed as mean ± S.E.

RESULTS

Peroxisome Targeting of the GFP-based Ca^{2+} Indicator—Fig. 1, *top*, shows the schematic structure of D3cpv, modified by the insertion at the C-terminal of the canonical peroxisomal targeting signal, the tripeptide Ser-Lys-Leu (*SKL*) (6). Although this sequence is known to be efficacious in targeting several recombinant proteins to peroxisomes, the D3cpv-SKL subcellular distribution (Fig. 1*A*) in HeLa cells transiently expressing the construct was indistinguishable from that of cytosolic D3cpv (Fig. 1*B*). Treatment of cells with digitonin, although releasing all cytosolic D3cpv (not shown), revealed that a fraction of the D3cpv-SKL was trapped in numerous small structures scattered throughout the cytoplasm (Fig. 1*C*). The D3cpv-SKL-positive spots coincide with peroxisomes, as revealed by their positivity after immunostaining with antibodies for markers of these organelles, catalase (Fig. 2*B*) or the peroxisomal membrane protein 70 (Fig. 2*E*). The missorting of D3cpv-SKL was observed in all other cell types investigated, GH3, Chinese hamster ovary, and SH-SY5Y. The cytoplasmic staining was not due to protein overexpression and saturation of the peroxisome protein import mechanism, because the same results were obtained when transfection was carried out with only 1/5 of the cDNA or if the cells were observed 48, 72, or 96 h after transfection (not shown).

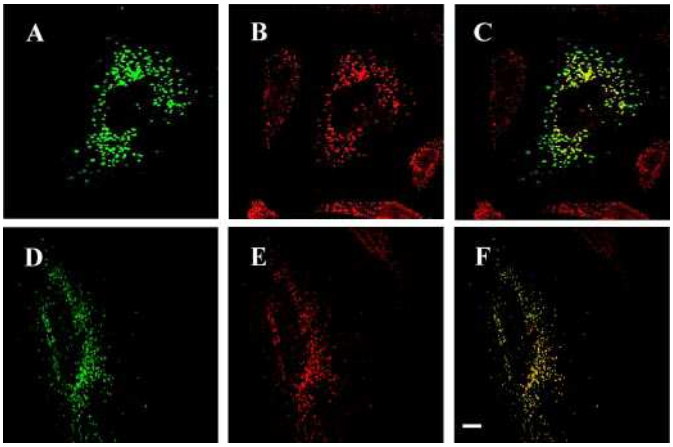

FIGURE 2. **D3cpv-SKL co-localizes after cell membrane permeabilization with the peroxisome protein markers, catalase and PMP70.** HeLa cells transiently expressing D3cpv-SKL were permeabilized with digitonin (*A* and *D*). Cells were then fixed and treated with an antibody against a peroxisome marker, catalase (*B*) or PMP70 (*E*) and then with a secondary antibody conjugated to Alexa 568. Co-localization of the two signals is shown in *C* and *F*. *Scale bar*, 10 μm.

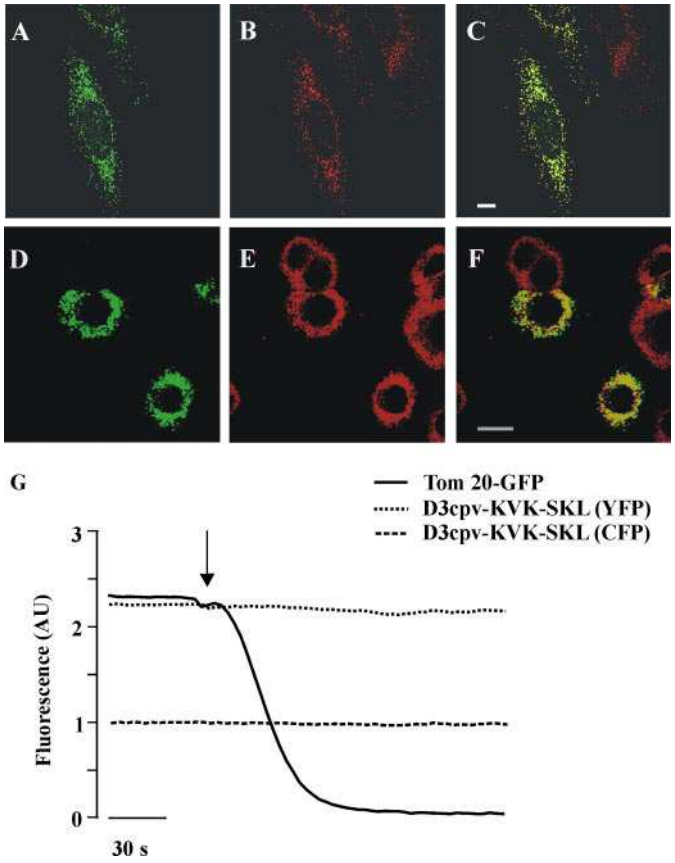

FIGURE 3. **Subcellular localization of transiently expressed D3cpv-KVK-SKL in HeLa and GH3 cells.** Confocal images of HeLa (*A*) or GH3 cells (*D*) transiently expressing D3cpv-KVK-SKL. In *B* and *E*, the immunolocalization of the peroxisome membrane protein PMP70 is presented. In *C* and *F*, the colocalization of the two signals is coded as *yellow*. For details, see "Materials and Methods." *Scale bar*, 10 μm. *G*, HeLa cells transiently expressing either D3cpv-KVK-SKL or TOM20-GFP, a fluorescent protein linked to the outer mitochondrial membrane and facing the cytosol, were permeabilized with digitonin in an intracellular-like medium and treated with proteinase K (see "Materials and Methods"). GFP fluorescence (*continuous trace*), yellow fluorescent protein fluorescence (*YFP*) (*dotted trace*), and cyan fluorescent protein fluorescence (*CFP*) (*dashed trace*) are presented (*AU*, arbitrary units). The *arrow* indicates Proteinase K addition. Similar experiments were carried out in GH3 cells with identical results.

To improve the peroxisome localization, a novel construct was made where the C-terminal SKL was preceded by a three-amino acid positively charged sequence, Lys-Val-Lys (KVK). This sequence was designed to fit the requirement for improved peroxisomal targeting described by Neuberger *et al.* (7, 8) (Fig. 3*A*). The majority of cells transfected with D3cpv-KVK-SKL were characterized by the presence only of punctate fluorescence, with a negligible signal in the cytosol. A small percentage of cells (5–30%) still revealed cytosol missorted probe. Such increase in targeting efficiency was observed also in Chinese hamster ovary, SH-SY5Y (not shown), and GH3 cells (Fig. 3*D*). Immunostaining with anti-PMP70 antibody revealed that all the D3cpv-KVK-SKL-positive vesicles of HeLa and GH3 cells are also positive for the *bona fide* peroxisome marker (Fig. 3, *C* and *F*).

The experiment presented in Fig. 3*G* was aimed at determining whether the Ca^{2+} probe was trapped within the peroxisome lumen or whether it was bound to the cytosolic surface of peroxisomes. The plasma membrane of HeLa cells was permeabilized with digitonin, and the cells were then treated with Proteinase K. The protease did not affect the D3cpv-KVK-SKL fluorescent signal, whereas, on the contrary, in cells expressing a GFP construct localized on the cytosolic surface of the outer mitochondrial membrane, TOM20-GFP (9), the enzyme abolished the fluorescence in a few seconds. Similar results were obtained in GH3 cells (not shown).

Ca^{2+} Handling by Peroxisomes in Intact Cells—We used as a first model system GH3 cells because these cells are endowed with (i) abundant plasma membrane voltage-gated Ca^{2+} channels and (ii) endogenous receptors (TRH receptors) coupled to inositol 1,4,5-trisphosphate production and Ca^{2+} mobilization from stores (10). Fig. 4*A* shows the typical response pattern of the D3cpv-KVK-SKL fluorescence signal of three GH3 cells to depolarization with 30 mM KCl. In two cells, the fluorescence was exclusively in peroxisomes, whereas in the third cell fluorescence was diffuse throughout the whole cytosol. Cell depolarization caused an increase in the fluorescence emitted at 540 nm and a decrease of the signal at 480 nm (not shown) and thus an increase in the 540/480-nm fluorescence emission ratio (here presented as $\Delta R/R_0$), which is proportional to $[Ca^{2+}]$ (Fig. 4*A*). The kinetics of the $\Delta R/R_0$ changes were, however, different in the cells where the probe was localized in the peroxisomes and in the cell with the mistargeted indicator. The cytosolic $\Delta R/R_0$ (*continuous line*) reached the peak in 1–2 s and then started to decrease slowly; the peroxisome signal, on the contrary, reached the peak in 10–15 s and then started to decline. Addition of EGTA accelerated the drop to basal level of both the cytosolic and peroxisomal signals, the effect on the cytosol being more evident. In Fig. 4*B*, the fluorescence emission ratio (excitation 340/380 nm) of a parallel batch of cells loaded with the Ca^{2+} indicator fura-2 is presented. The kinetics of the fura-2 signal were similar to that of cells expressing the missorted D3cpv-KVK-SKL probe (Fig. 4*A*). Similar data were obtained with cells expressing the original cytosolic D3cpv (not shown). In the experiment presented in Fig. 4*C* the peak levels reached by $[Ca^{2+}]_p$, expressed as percentage of the maximal

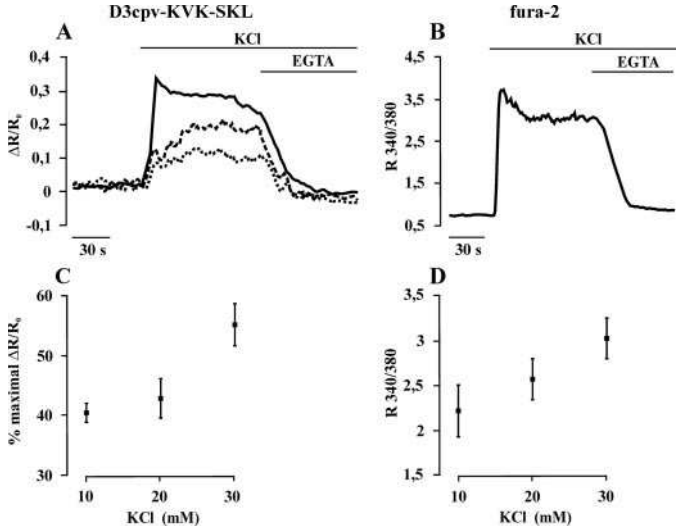

FIGURE 4. **Peroxisome Ca^{2+} increases in GH3 cells.** Kinetics of the fluorescence changes of typical GH3 cells transiently expressing (i) D3cpv-KVK-SKL, selectively within peroxisomes (*A*, two cells, *dashed* and *dotted traces*), (ii) mistargeted to the cytosol (*A*, *continuous trace*), or (iii) loaded with fura-2 (*B*). Where indicated, 30 mM KCl and 2 mM EGTA were added in a Ca^{2+}-containing medium. When 30 mM NaCl was added instead of KCl, no effect on either cytosolic or peroxisomal $[Ca^{2+}]$ was recorded. Data are plotted as $\Delta R/R_0$, where R_0 is the fluorescence emission ratio (*R* 540/480 nm) at time 0 and ΔR is the increase in fluorescence emission ratio at any point. For fura-2 measurements, the ratio of the light intensity emitted at 505 nm upon dye excitation at the two wavelengths (*R* 340/380) is a function of the cytosolic $[Ca^{2+}]$ and is displayed on the *left side* of the panel in this and the following figures. *D*, mean rises in the *R* 340/380-nm fluorescence excitation ratio of the fura-2 signal as a function of KCl concentration. The mean rises in peroxisome Ca^{2+} level (*C*), expressed as percentage of the 540/480 maximal $\Delta R/R_0$, show a similar trend. Mean of 15 (*C*) or 19 (*D*) experiments ± S.E. For details, see "Materials and Methods."

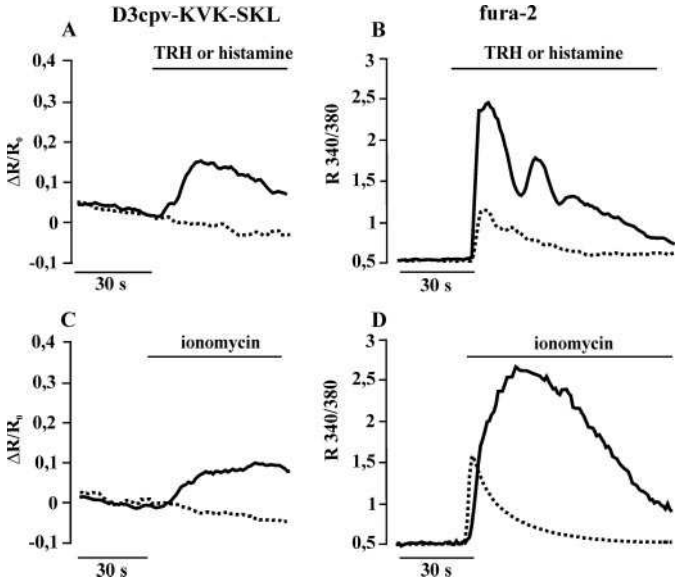

FIGURE 5. **Ca^{2+} release from stores causes a peroxisomal Ca^{2+} rise in HeLa, but not in GH3, cells.** Kinetics of the fluorescence changes of a typical HeLa cell (*continuous trace*) or GH3 cell (*dotted trace*) transiently expressing D3cpv-KVK-SKL in peroxisomes (*A* and *C*) or loaded with fura-2 (*B* and *D*). Where indicated, ionomycin (100 nM), the inositol 1,4,5-trisphosphate-generating agonist histamine (100 μM), for HeLa cells, or TRH (1 μM) for GH3 cells was added in a Ca^{2+}-free medium. For details, see "Materials and Methods."

$\Delta R/R_0$, are plotted as a function of KCl concentration. For comparison, in Fig. 4*D* the 340/380 nm emission ratio of cells loaded with fura-2 is also shown. It is clear that the peak rise in peroxisomal and fura-2 signals showed a similar dependence on [KCl]. Confirming that the $[Ca^{2+}]_p$ increase depends on the cytosolic $[Ca^{2+}]$ rise, when KCl was added in a medium devoid of Ca^{2+} no increase in peroxisome and cytosolic $[Ca^{2+}]$ was observed (not shown).

The question then arises as to the behavior of peroxisomes, in terms of Ca^{2+} response, to agents that cause Ca^{2+} mobilization from intracellular stores, either elicited by TRH or by the Ca^{2+} ionophore ionomycin, both added in the absence of extracellular Ca^{2+}. The two agents caused neither a drop nor a rise in $[Ca^{2+}]_p$ (under conditions that elicited significant transient Ca^{2+} rises, as measured with fura-2; compare Fig. 5, *A* and *C*, with Fig. 5, *B* and *D*, *dotted traces*). When TRH or ionomycin was added after a previous pulse of KCl (to overload Ca^{2+} stores), the percentage of peroxisomal Ca^{2+} increases in response to TRH and ionomycin increased significantly (20 and 53% of cells, respectively; not shown). The problem of the peroxisomal behavior in response to Ca^{2+}-mobilizing stimuli was then further addressed in HeLa cells treated with histamine or ionomycin (Fig. 5). In all cells investigated, histamine induced a cytosolic $[Ca^{2+}]$ rise, as measured with fura-2 (Fig. 5*B*, *continuous trace*), whereas in 68% of cells the peroxisome signal also increased significantly (Fig. 5*A*, *continuous trace*). In HeLa cells, addition of ionomycin in Ca^{2+}-free medium (which resulted in a large cytosolic $[Ca^{2+}]$ increase in all cells tested; Fig. 5*D*, *continuous trace*) always resulted in a rise of $[Ca^{2+}]_p$ (Fig. 5*C*, *continuous trace*).

Mechanism of Ca^{2+} Transport in Peroxisomes—The Ca^{2+} rise within peroxisomes induced by KCl-dependent depolarization in GH3 cells was indistinguishable in the presence or absence of mitochondrial uncouplers or of sarcoendoplasmic reticulum Ca^{2+} ATPase inhibitors (not shown). Given that no reliable inhibitor of the Golgi-type pump is available, to verify the involvement of ATP-dependent uptake mechanisms we investigated the effects of ATP on the rate and extent of $[Ca^{2+}]_p$ rise in digitonin-permeabilized cells exposed to a medium with 500 nM Ca^{2+}. As shown in Fig. 6*A*, Ca^{2+} uptake was similar with (*continuous trace*) and without (*dotted trace*) an energy source. Notably, when an excess EGTA was added (to rapidly decrease medium $[Ca^{2+}]$), the peroxisome $[Ca^{2+}]$ decreased with relatively slow kinetics (Fig. 6*B*) To test whether peroxisomal Ca^{2+} influx depends on the presence of a classical Ca^{2+} channel, digitonin-permeabilized cells were treated with 10 μM La^{3+}, a nonspecific inhibitor of several Ca^{2+} channels. The increase in $[Ca^{2+}]_p$ upon increase in medium $[Ca^{2+}]$ to 500 nM or 5 μM was unaffected by La^{3+} (not shown).

We then investigated whether peroxisomal Ca^{2+} uptake may depend on a $Na^+(H^+)/Ca^{2+}$ antiport. Intact GH3 cells were pretreated with either NH_4Cl (Fig. 6*C*, *dotted trace*), an agent that causes an alkalinization of organelle pH, or monensin (*dashed trace*), a H^+/Na^+ exchange ionophore, which should collapse any gradient of either Na^+ or H^+ across the peroxisomal membrane, if they exist. Neither NH_4Cl nor monensin had any appreciable effect on the $[Ca^{2+}]_p$ increase caused by 30 mM KCl. Similar results were obtained in HeLa cells stimulated with either histamine or ionomycin (not shown).

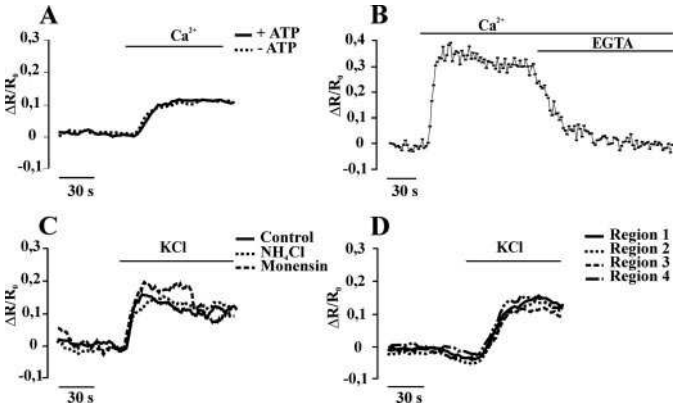

FIGURE 6. **Effects of ATP, H^+, or Na^+ gradients on peroxisomal Ca^{2+} uptake in GH3 cells and homogeneous responses of peroxisomes within a cell to a cytosolic Ca^{2+} rise.** *A*, GH3 cells transiently expressing D3cpv-KVK-SKL were permeabilized with digitonin in an intracellular-like medium, described under "Materials and Methods," with (*continuous trace*) or without (*dotted trace*) 200 μM ATP and 2 mM succinate. After digitonin washout, the cells were superfused with medium whose $[Ca^{2+}]$ was buffered at 500 nM. *B*, the same conditions as *A* where indicated 150 μM Ca^{2+} and 250 μM EGTA were added. *C*, intact GH3 cells expressing D3cpv-KVK-SKL selectively in peroxisomes were treated with 10 mM NH_4Cl (*dotted trace*) or 5 μM monensin (*dashed trace*) 30 s before inducing depolarization with 30 mM KCl. *D*, kinetic changes of $\Delta R/R_0$ of four different groups of peroxisomes within the same GH3 cell are presented. Cell was stimulated with 30 mM KCl in a Ca^{2+}-containing medium.

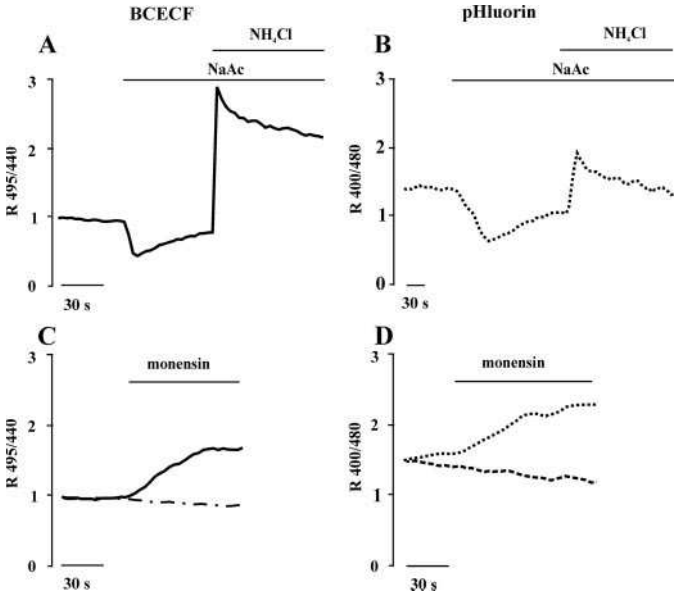

FIGURE 7. **Measurement of peroxisome luminal pH.** GH3 cells loaded with the cytosolic pH indicator BCECF (*A* and *C*) or transiently expressing the peroxisomal pH probe pHluorin (*B* and *D*) were challenged where indicated with $NaCH_3CO_2$ (NaAc, 30 mM), NH_4Cl (30 mM), or monensin (5 μM) in a Ca^{2+}-containing medium. For *C* and *D* (*dashed-dot* and *dashed traces*), the pH of the extracellular medium was decreased to 7.0, NaCl was iso-osmotically substituted with KCl, $CaCl_2$ was omitted, and 100 μM EGTA was added instead. For further details, see "Materials and Methods."

To verify whether there are heterogeneities among the organelles, the $[Ca^{2+}]$ rise in different groups of peroxisomes was next investigated. As shown in Fig. 6*D*, the response to a 30-mM KCl challenge of different groups of organelles within the same GH3 cell was found to be very similar. Identical results were obtained in HeLa cells using either ionomycin or histamine as the stimulus (not shown).

Finally, the peroxisome lumenal pH was directly monitored using the targeted pH indicator pHluorin (see "Materials and Methods" and Ref. 11). Cytosolic pH was measured in parallel with BCECF (12). Fig. 7 shows that the weak acid acetate caused a reduction of both cytoplasmic (Fig. 7*A*) and peroxisomal (Fig. 7*B*) pH, whereas NH_4Cl caused an alkalinization of both compartments. Monensin also caused an increase of pH both in the cytosol (Fig. 7*C*, *continuos trace*) and in peroxisomes (Fig. 7*D*, *dotted trace*). When the cells were incubated in a medium where NaCl was iso-osmotically substituted with KCl (to abolish the Na^+ gradient across the plasma membrane and in the absence of Ca^{2+} to block Ca^{2+} influx) and the extracellular pH was dropped to 7.0 (to reduce the pH gradient), monensin hardly modified cytosolic pH (Fig. 7*C*, *dashed point trace*) and in parallel failed to cause any significant change in peroxisomal pH (Fig. 7*D*, *dashed trace*).

Calibration of the Peroxisomal $[Ca^{2+}]$—To determine the absolute values of $[Ca^{2+}]_p$, the *in situ* K_d for Ca^{2+} of D3cpv-KVK-SKL was determined using the passive Ca^{2+} loading procedure previously described (13). Transfected cells were permeabilized with digitonin in an intracellular-like medium, but devoid of ATP or any mitochondrial oxidizable substrate, and variable concentration of Ca^{2+} (see "Materials and Methods"). The percentage of the normalized 540/480-nm fluorescence emission ratio changes at steady state were then plotted as a function of medium $[Ca^{2+}]$ (Fig. 8). The apparent K_d for Ca^{2+},

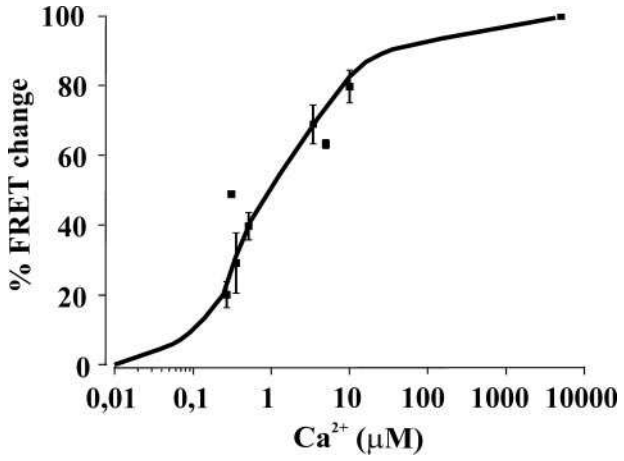

FIGURE 8. ***In situ* calibration of D3cpv-KVK-SKL fluorescence as a function of $[Ca^{2+}]$.** GH3 cells transiently expressing D3cpv-KVK-SKL were permeabilized with digitonin in an intracellular-like medium supplemented with 100 μM EGTA and devoid of ATP and succinate. The value of 540/480 nm fluorescence emission ratio under these conditions was assumed to represent R_{min}. The cells were then superfused with medium whose $[Ca^{2+}]$ was buffered (with EGTA) at different levels up to a concentration of 3 μM Ca^{2+}. The values of $[Ca^{2+}]$ above 3 μM were obtained by simply adding $CaCl_2$ at the indicated concentrations to medium without EGTA. R_{max} was determined by addition of 5 mM $CaCl_2$. As described in the supplemental material, the values of *R* at the different Ca^{2+} concentration of independent experiments were normalized based on the observation that the R_{max}/R_{min} ratio is constant in different cells. The normalized *R* values (mean ± S.E.) were then plotted as a function of the $[Ca^{2+}]$ ($n = 37$).

as calculated *in situ*, 1.0 μM, is not much different from that calculated *in vitro* with recombinant D3cpv, 0.6 μM (5). A detailed description of the protocol employed to calculate the $[Ca^{2+}]$ within peroxisomes is presented in supplemental data. A summary of the absolute values of $[Ca^{2+}]_p$ (as measured with D3cpv-KVK-SKL), compared with the cytosolic Ca^{2+} values (as

TABLE 1
$[Ca^{2+}]$ in cytosol and peroxisome lumen upon addition of different stimuli

Conditions as in Figs. 5 and 6. Mean of 61 (*fura-2*) and 38 (*D3cpv-KVK-SKL*) experiments ± S.E.

Stimulus	Cell type	Ca^{2+} fura-2	S.E.	Ca^{2+} D3cpv-KVK-SKL	S.E.
		μM	μM	μM	μM
KCl (10 mM)	GH3	1.79	0.47	0.52	0.08
KCl (20 mM)	GH3	2.01	0.41	0.64	0.10
KCl (30 mM)	GH3	3.34	0.84	1.32	0.25
histamine (100 μM)	HeLa	1.31	0.13	0.72	0.11
Ionomycin (100 nM)	HeLa	1.33	0.59	0.76	0.11

measured in parallel by fura-2), is presented in Table 1. The $[Ca^{2+}]_p$ at rest, both in HeLa and GH3 cells, is ~150 nM, *i.e.* not significantly different from that measured with fura-2 (150 and 190 nM for GH3 and HeLa cells, respectively). The mean $[Ca^{2+}]_p$ peak of GH3 cells (upon stimulation with 30 mM KCl), 1.32 ± 0.25 μM, compares to 3.34 ± 0.84 μM measured with fura-2. The averaged $[Ca^{2+}]_p$ peaks in HeLa cells stimulated with histamine or ionomycin (both added in Ca^{2+}-free medium) are 0.72 ± 0.11 and 0.76 ± 0.11 μM compared with cytosolic peaks of 1.31 ± 0.13 and 1.33 ± 0.59 μM, respectively.

DISCUSSION

The most common peroxisome-targeting mechanism involves the C terminus tripeptide SKL (6). When this sequence was added to the GFP-based Ca^{2+} indicators D1- and D3cpv (5) most of the transfected protein mislocalized to the cytosol. Inclusion of a longer targeting sequence (KVK-SKL), however, resulted in more satisfactory peroxisome localization. The expressed protein is clearly trapped in the lumen of the organelles, as demonstrated by its resistance to proteolytic cleavage and by the slower kinetics of the fluorescence signal changes in response to a sudden change in extraperoxisomal $[Ca^{2+}]$.

When cytosolic $[Ca^{2+}]$ was increased in GH3 cells by depolarizing the plasma membrane with high KCl, the $[Ca^{2+}]_p$ also raised, although with slower kinetics. The amplitude of the $[Ca^{2+}]_p$ increase paralleled that of the cytosol. In quantitative terms, the maximum rises of $[Ca^{2+}]_p$ after depolarization were lower than those calculated with the classical cytosolic indicator fura-2. Considering the inherent assumptions involved in the calibration procedures of the two probes, it can be safely concluded that $[Ca^{2+}]_p$ tends to equilibrate with the cytosolic $[Ca^{2+}]$ and no driving force (ATP and/or $Na^+(H^+)$ gradients) leads to Ca^{2+} influx into peroxisomes. In support of this conclusion, the luminal pH of peroxisomes is practically indistinguishable from that of the cytoplasm, and monensin never caused an acidification of peroxisomal lumen, demonstrating that $[Na^+]$ of peroxisomes is similar to that of cytoplasm. Our conclusion concerning the lack of any significant gradient of H^+ across the peroxisomal membrane concurs with Jankowski *et al.* (11), whereas other groups have reported that the intraperoxisome pH is slightly alkaline in mammalian cells (14) or in yeasts slightly acidic (15) or alkaline (16, 17).

A permeability barrier to Ca^{2+} diffusion across the peroxisome membrane, however, does exist as demonstrated by these results: (i) the rate of peroxisome Ca^{2+} rise in intact cells treated with KCl is substantially slower than in the cytosol, and (ii) in permeabilized cells, sudden changes in medium $[Ca^{2+}]$ require several seconds to equilibrate with the organelle lumen. Surprisingly, whereas increases in cytosolic $[Ca^{2+}]$ elicited in GH3 cells by Ca^{2+} influx though voltage-gated Ca^{2+} channels were followed by $[Ca^{2+}]_p$ rises, Ca^{2+} mobilization from internal stores, as induced by stimulation of TRH receptors, almost never resulted in a significant increase in $[Ca^{2+}]_p$. Even unspecific Ca^{2+} mobilization from stores, as promoted by ionomycin added in Ca^{2+}-free medium, was unable to induce Ca^{2+} uptake into peroxisomes of GH3 cells. The possibility was thus considered that the poor response of the peroxisomes to Ca^{2+} mobilization in GH3 cells reflects (i) the existence of a mechanism that prevents Ca^{2+} uptake in peroxisomes in response to Ca^{2+} mobilization from stores or (ii) a combination of the small and transient nature of the cytosolic Ca^{2+} rise in response to TRH (and ionomycin) in GH3 cells and of the slow Ca^{2+} uptake rate by peroxisomes. In other words, the small and transient rise in cytosolic $[Ca^{2+}]$ (as that elicited in GH3 cells by TRH or ionomycin) can be hardly coped with by the relatively slow Ca^{2+} uptake system of peroxisomes. The cytoplasmic $[Ca^{2+}]$ rise in response to depolarization, instead, does reach the peak in 2–3 s, but it is followed by a prolonged plateau level that lasts several tens of seconds. In support of the latter explanation, the very rapid Ca^{2+} increases due to spontaneous action potential firing (and Ca^{2+} influx through voltage-gated Ca^{2+} channels) often observed in GH3 cells (18) were never followed by significant increases in $[Ca^{2+}]_p$.

To distinguish between these possibilities, we used a different cell type, HeLa, where Ca^{2+} mobilization from stores in response to an inositol 1,4,5-trisphosphate-generating agonist, such as histamine, results in larger and relatively more prolonged Ca^{2+} transients compared with GH3 cells (peak values measured with fura-2 of 1.31 μM and 270 nM, back to basal levels in 120 and 50 s, in HeLa and GH3 cells, respectively). Indeed, we found that in HeLa cells the percentage of peroxisome responses to histamine application was much higher than that observed in GH3 cells in response to TRH (68 *versus* 1%, respectively) and the percentage of $[Ca^{2+}]_p$ increases in response to ionomycin was close to 100% in HeLa cells compared with <5% in GH3 cells. Thus, it may be concluded that, due to the intrinsic sluggish response to a cytosolic Ca^{2+} rise, peroxisomes are relatively insensitive to rapid transients of cytosolic $[Ca^{2+}]$ but significantly increase their Ca^{2+} level only in response to prolonged cellular Ca^{2+} increases. We cannot exclude, however, that peroxisomes of HeLa cells are more efficient than those of GH3 cells at taking up Ca^{2+}. However, when in GH3 cells TRH- or ionomycin-induced cytosolic Ca^{2+} increases are larger and more prolonged (as occurs when they are applied after KCl), the percentage of peroxisomal responses increases drastically (from 1 to 21% for TRH and from 5 to 53% with ionomycin), suggesting that the first explanation is most likely.

The final question concerns the heterogeneity of peroxisomal Ca^{2+} responses. When groups of organelles in the same cell were compared, no significant difference, either in kinetics or in amplitude of the Ca^{2+} responses, was ever observed. It cannot

be excluded, however, that single organelles localized in the proximity of Ca^{2+} channels of either the plasma membrane or the endoplasmic reticulum may experience larger local Ca^{2+} rises and, accordingly, undergo larger Ca^{2+} increases.

In conclusion, we have developed novel GFP-based Ca^{2+} indicators that can efficiently target to the peroxisomal lumen. These allow, for the first time to our knowledge, the measurement of this parameter in intact living cells. Taken together, the present data demonstrate that peroxisomes participate in the Ca^{2+} signaling pathway but their behavior is unlike that of any other organelle. In particular, peroxisomes do not act as Ca^{2+} stores from which Ca^{2+} can be mobilized upon stimulation, as the endoplasmic reticulum, the Golgi apparatus or, in some cells, acidic compartments (19). The Ca^{2+} response of peroxisomes to a rise in cytosolic $[Ca^{2+}]$ is also markedly different from that of mitochondria, in as much as their luminal Ca^{2+} does not increase as massively as that of the latter organelles. The organelle that most resembles peroxisomes in terms of Ca^{2+} response is the nucleus, although in the latter the kinetics of Ca^{2+} equilibration with the cytosol are 10–100-fold faster. Thus, because of this relatively slow Ca^{2+} influx, very rapid and transient increases in cytosolic Ca^{2+} may not lead to appreciable changes in $[Ca^{2+}]_p$, whereas more sustained increases will always lead to an increase in $[Ca^{2+}]_p$. It remains to be established whether and which reactions within the peroxisomes are affected by Ca^{2+}.

The amount of Ca^{2+} that is sequestered by peroxisomes will depend on (i) their number and volume (which may vary among different cells and in response to specific stimuli, *e.g.* peroxisome proliferator-activated receptor γ gene activation) and (ii) the endogenous Ca^{2+} buffering capacity of the organelles, which is presently unknown. In addition to a potential role as a cytosolic Ca^{2+} buffer, the increases in $[Ca^{2+}]_p$ may be relevant for the organelle's own functions. Thus far, potential candidates are the peroxisomal Ca^{2+}-dependent members of the mitochondrial carrier superfamily that contains four EF-hand Ca^{2+} binding domains (20) or a Ca^{2+}/calmodulin-regulated catalase isoform found in plant peroxisomes (21). The search for Ca^{2+}-modulated peroxisomal proteins may now be launched on a firmer ground, given the direct demonstration of the participation of these organelles in cellular Ca^{2+} handling.

Acknowledgment—We thank Paulo Magalhães for critically reading the manuscript and Paul Lazarow for helpful discussion.

REFERENCES

1. Platta, H. W., and Erdmann, R. (2007) *Trends Cell Biol.* **17,** 474–484
2. Poirier, Y., Antonenkov, V. D., Glumoff, T., and Hiltunen, J. K. (2006) *Biochim. Biophys. Acta* **1763,** 1413–1426
3. Goepfert, S., and Poirier, Y. (2007) *Curr. Opin. Plant Biol.* **10,** 245–251
4. Shimozawa, N. (2007) *J. Inherit. Metab. Dis.* **30,** 193–197
5. Palmer, A. E., Giacomello, M., Kortemme, T., Hires, S. A., Lev-Ram, V., Baker, D., and Tsien, R. Y. (2006) *Chem. Biol.* **13,** 521–530
6. Gould, S. J., Keller, G. A., Hosken, N., Wilkinson, J., and Subramani, S. (1989) *J. Cell Biol.* **108,** 1657–1664
7. Neuberger, G., Maurer-Stroh, S., Eisenhaber, B., Hartig, A., and Eisenhaber, F. (2003) *J. Mol. Biol.* **328,** 567–579
8. Neuberger, G., Maurer-Stroh, S., Eisenhaber, B., Hartig, A., and Eisenhaber, F. (2003) *J. Mol. Biol.* **328,** 581–592
9. Kanaji, S., Iwahashi, J., Kida, Y., Sakaguchi, M., and Mihara, K. (2000) *J. Cell Biol.* **151,** 277–288
10. Pizzo, P., Fasolato, C., and Pozzan, T. (1997) *J. Cell Biol.* **138,** 355–366
11. Jankowski, A., Kim, J. H., Collins, R. F., Daneman, R., Walton, P., and Grinstein, S. (2001) *J. Biol. Chem.* **276,** 48748–48753
12. Tsien, R. Y., Pozzan, T., and Rink, T. J. (1982) *J. Cell Biol.* **94,** 325–334
13. Rudolf, R., Magalhaes, P. J., and Pozzan, T. (2006) *J. Cell Biol.* **173,** 187–193
14. Dansen, T. B., Wirtz, K. W., Wanders, R. J., and Pap, E. H. (2000) *Nat. Cell Biol.* **2,** 51–53
15. Lasorsa, F. M., Scarcia, P., Erdmann, R., Palmieri, F., Rottensteiner, H., and Palmieri, L. (2004) *Biochem. J.* **381,** 581–585
16. Waterham, H. R., Keizer-Gunnink, I., Goodman, J. M., Harder, W., and Veenhuis, M. (1990) *FEBS Lett.* **262,** 17–19
17. van Roermund, C. W., de Jong, M., IJlst, L., van Marle, J., Dansen, T. B., Wanders, R. J., and Waterham, H. R. (2004) *J. Cell Sci.* **117,** 4231–4237
18. Schlegel, W., Winiger, B. P., Mollard, P., Vacher, P., Wuarin, F., Zahnd, G. R., Wollheim, C. B., and Dufy, B. (1987) *Nature* **329,** 719–721
19. Rizzuto, R., and Pozzan, T. (2006) *Physiol. Rev.* **86,** 369–408
20. Weber, F. E., Minestrini, G., Dyer, J. H., Werder, M., Boffelli, D., Compassi, S., Wehrli, E., Thomas, R. M., Schulthess, G., and Hauser, H. (1997) *Proc. Natl. Acad. Sci. U. S. A.* **94,** 8509–8514
21. Yang, T., and Poovaiah, B. W. (2002) *Proc. Natl. Acad. Sci. U. S. A.* **99,** 4097–4102

SUPPLEMENTAL DATA

Calibration of the 540/480 nm fluorescence ratio in terms of absolute peroxisome [Ca^{2+}]- Determination of the K_d for Ca^{2+} of peroxisome-targeted D3cpv-KVK-SKL was carried out essentially as described previously by passive Ca^{2+} loading in digitonin-permeabilized cells (1). We found that the 540/480 nm fluorescence ratio in the peroxisome lumen was variable among different cells (both in intact resting cells and after permeabilization in medium with [Ca^{2+}] < 1 nM). As shown in Fig. S1, the 540/480 nm fluorescence emission ratio (both in resting cells and after permeabilization with digitonin in low-Ca^{2+} medium) increased as the absolute level of fluorescence increased. In particular, the fluorescence emission at 540 nm increased more than that at 480 nm, suggesting the existence of Ca^{2+}-independent FRET. The simplest explanation for this finding is that the higher the concentration of the probe, the higher the probability that two indicator molecules interact within peroxisomes and give rise to a Ca^{2+}-independent FRET. However, the ratio between the maximal 540/480 nm fluorescence ratio, R_{max}, (obtained by adding 5 mM $CaCl_2$) and R_{min} (at <1 nM Ca^{2+}) was constant, 1.41 ± 0.03, thus allowing the normalization of values for different cells. The calibration was thus carried out by exposing the permeabilized cells to media whose [Ca^{2+}] was buffered at different levels until the ratio signal stabilized at a new level. The percentages of the normalized 540/480 fluorescence emission ratio changes were then plotted against the [Ca^{2+}] to obtain the calibration curve shown in Fig. 8.

In order to determine the [Ca^{2+}] within peroxisomes of intact cells, the minimal and maximal 540/480 nm fluorescence emission ratio, R_{min} and R_{max}, were also calculated in living cells. In intact cells, the R_{min} was determined by incubating the cells in a Ca^{2+}-free medium (+ EGTA) and loaded with BAPTA/AM, a condition that is known to cause a reduction of both cytosolic and organelle [Ca^{2+}] to below 5 nM (2). The value of R_{min} thus obtained was indistinguishable from that obtained after permeabilization in medium with [Ca^{2+}] <1nM. The R_{max} was obtained by adding M□5 ionomycin and 10 mM $CaCl_2$ and was not different from that obtained in permeabilized cells exposed to 5 mM $CaCl_2$.

The absolute value of the 540/480 nm fluorescence emission ratio of D3cpv (cytosolic) was lower than the 540/480 nm fluorescence ratio of the same probe in peroxisomes (or when missorted in the cytosol). This is most likely due to the Ca^{2+}-independent FRET described above and not to a difference in the resting value of [Ca^{2+}] between the two compartments, because: i) in cells loaded with BAPTA in Ca^{2+}-free medium

(+EGTA), the difference of the 540/480 nm fluorescence emission ratio between peroxisomes and cytosol was maintained; ii) as mentioned above, the 540/480 nm fluorescence emission ratio at rest was similar whether measured in intact cells or after plasma membrane permeabilization with digitonin, in a medium devoid of any energy source and with a $[Ca^{2+}]$ below 10^{-9} M

Calibration of the fura-2 signal in terms of $[Ca^{2+}]$ was carried out essentially as described for D3cpv-KVK-SKL, assuming a K_d for Ca^{2+} of 224 nM.

SUPPLEMENTAL FIGURE

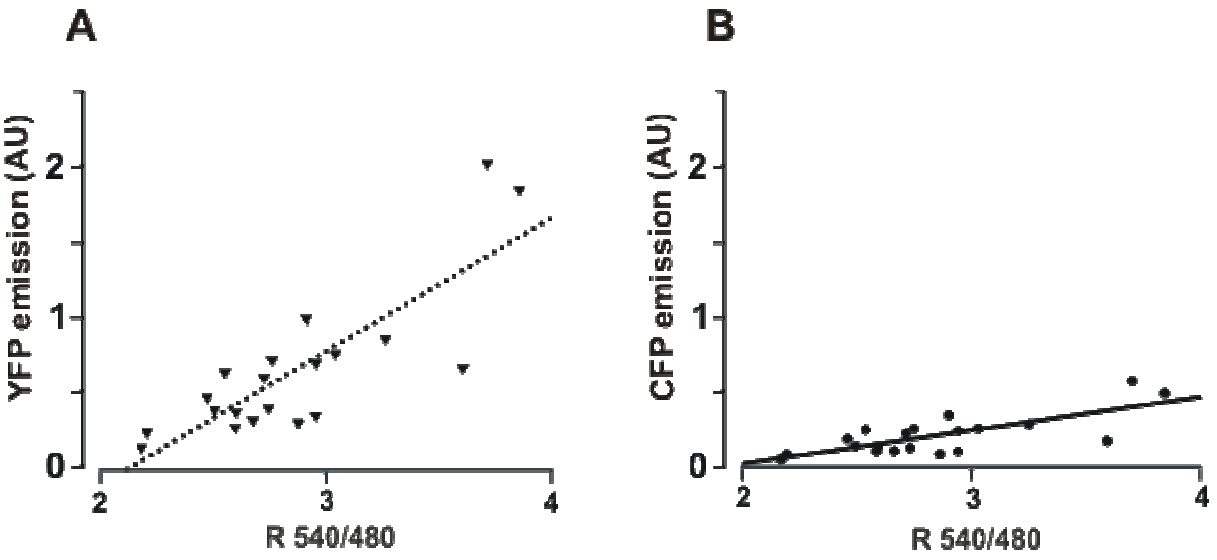

Figure S1

SUPPLEMENTAL FIGURE LEGEND

Fig. S1. Ca^{2+} independent FRET. The intensities of the fluorescence emission of YFP (A) or CFP (B) (arbitrary units, AU) upon 425 nm excitation in different HeLa cells were plotted as a function of the corresponding 540/480 fluorescence emission ratio (N= 20).

SUPPLEMENTAL REFERENCES

1. Rudolf, R., Magalhaes, P. J., and Pozzan, T. (2006) *Journal of Cell Biology* **173**, 187-193
2. Arslan, P., Di Virgilio, F., Beltrame, M., Tsien, R. Y., and Pozzan, T. (1985) *Journal of Biological Chemistry* **260**, 2719-2727

5.2 Supplemental discussion

Recent findings have rule out the established idea that peroxisomal membrane is freely permeable to small metabolites and ions (Introduction, § 1.4). Moreover, several studies have demonstrated that peroxisomes are not only the "biochemical station" of the cell, but they can also take part in different signalling pathways and are strictly related to other subcellular compartments like ER or mitochondria (Camoes et al., 2008). Surprisingly, up to few months ago, there was no information available about a possible role of peroxisomes in cellular Ca^{2+} handling. More surprising was the publication at few days of distance of two papers concerning the same issue that was addressed by the use of two different genetically encoded Ca^{2+} probes. Lasorsa and colleagues took advantage of the chemiluminescent protein aequorin by targeting it into peroxisomal lumen thanks to the classical PTS SKL (Lasorsa et al., 2008). They found that upon cellular stimulation with an IP3-coupled agonist peroxisomes can reach Ca^{2+} peaks up to 50-100 μM, with a fast kinetic very similar to mitochondrial one. Peroxisomal Ca^{2+} peaks and kinetic registered by peroxisomal aequorin are very different if compared to those registered with the peroxisomal camelon D3cpv-KVK-SKL, and so was the pharmacological sensitivity of this phenomenon. Peroxisomal Ca^{2+} entry seems in this case to be driven both by a H^+ and a Na^+ gradient, since treatments with agents that dissipate them (notably, FCCP and monensin) cause its inhibition. Measurement with peroxisomal aequorin revealed also the existence of a luminal Ca^{2+} gradient in resting condition. $[Ca^{2+}]$ within peroxisomal matrix is 20-fold higher than that measured in the cytosol, and the mechanism that allows this accumulation seems to be a V-type ATP-ase, since it is inhibited by bafilomycin.

These results are in contrast with those reported by D3cpv-KVK-SKL and a simple explanation for these differences is difficult to find. Firstly, we excluded a cell-specific peroxisomal Ca^{2+} dynamic: experiments performed with D3cpv-KVK-SKL in CHO cells, that with HeLa cells constitute the experimental model choosen by Lasorsa et al., revealed no difference if compared to what already reported in other cell types with this probe, that is, a slow equilibration of peroxisomal lumen with cytosolic Ca^{2+} upon cellular stimulation (data not shown). Secondly, even if we have already performed an *in situ* calibration of D3cpv-KVK-SKL demonstrating that the probe is not saturated, we performed the same experiments and *in situ* calibration in D1cpv-KVK-SKL expressing cells. This probe has two K_ds for Ca^{2+}, one of high Ca^{2+} affinity and a second one of lower affinity (1 and 60 μM, respectively), thus allowing the measurement of $[Ca^{2+}]$ in a broader range of $[Ca^{2+}]$ if compared to D3cpv. The

results obtained with this second probe confirmed what already seen in D3cpv-KVK-SKL expressing cells, i.e. that peroxisome [Ca^{2+}] is in equilibrium, at rest and during stimulation, with cytosolic [Ca^{2+}] (data not shown). The only explanation for the differences between our findings and those reported by Lasorsa et al. seems to be the existence of functionally different subpopulations of peroxisomes. This hypothesis is supported both from early observations and recent findings. The existence of subpopulations of peroxisomes that differ in their enzymatic content is established (Völkl et al., 1999). Moreover, Neuspiel et al. have recently demonstrated the existence of mitochondria-derived vesicles that detach from mitochondria and fuse with a subpopulation of peroxisomes, thus highlighting the heterogeneity of this organelle (Neuspiel et al., 2008). It is thus likely that peroxisomal cameleon and aequorin are preferentially targeted or at least their signal is dominated by one of these subpopulations.

PART II

Ca^{2+} homeostasis in plant peroxisomes

INTRODUCTION

6.1 Ca^{2+} signalling in plants

Ca^{2+} exerts a dual role in plants, since it constitutes a plant nutrient but it also covers structural roles in the cell wall and membrane, functions as counter-cation for inorganic and organic anions in the vacuole, and, last but not least, functions as intracellular messenger (White and Broadley, 2003).

Intracellular signalling requires $[Ca^{2+}]c$ to be maintained at submicromolar levels in resting conditions (as in animal cells) and to be rapidly increased in response to environmental stress or developmental cues. Plant cells are endowed with Ca^{2+}-ATPases and H^+/Ca^{2+} antiporters that remove cytosolic Ca^{2+} to either the apoplast (that is the space outside the plasma membrane) or the lumen of intracellular organelles, like the vacuole or the ER. By removing Ca^{2+} from the cytoplasm these enzymes maintain a low $[Ca^{2+}]c$ in unstimulated cells and restore the basal conditions following a perturbation, thereby influencing the magnitude, kinetics and subcellular distribution of cytosolic Ca^{2+} signals. They also replenish intracellular and extracellular Ca^{2+} stores and provide Ca^{2+} to the ER and secretory system. Ca^{2+} influx into the cytosol is mediated by different Ca^{2+} channels that usually are classified on the basis of their voltage dependence.

The three classes of cation channels are: depolarization-activated (DACC), hyperpolarization-activated (HACC) and voltage-independent (VICC). The principal role of these channels is to function in cell signalling, even if they can open in order to contribute to nutritional Ca^{2+} fluxes in certain cell types (White et al., 2000). All these channels are permeable to both monovalent and divalent cations contributing to the uptake of essential, but also toxic cations in addition to Ca^{2+}.

Most DACCs activate significantly at voltage more positive than about -150 mV to -100 mV under physiological conditions. Since plasma membrane depolarization is common to many stimuli, DACCs generally transduce stress-related signals. The outward rectifying K^+-channels found in the plasma membrane of plant cells are also Ca^{2+} permeable DACCs. They activate significantly at voltages more positive than -50 mV under physiological conditions and allow a large efflux of K^+ together with a smaller Ca^{2+} entry (Roberts and Snowman, 2000). This Ca^{2+} influx is thought to be fundamental in coordinate ion transport, metabolism and gene expression.

HACCs are permeable to different cations including Ca^{2+}, Ba^{2+}, Mg^{2+} and others, they activate at voltages more negative than about -100 mV and -150 mV at physiological $[Ca^{2+}]c$, but

increasing $[Ca^{2+}]c$ shifts their activation potential to more positive or negative voltages depending on cell type (Hamilton et al., 2000). These channels are also activated by reactive oxygen species (ROS) in different cell types (Pei et al., 2000; Demidchik et al., 2007). Two types of HACCs are also known to be located in plant vacuoles (White et al., 2000).

Many distinct VICCs are present in plasma membrane of plant cells. The features shared among them are the permeability to both mono- and divalent cation and the activation at physiological voltages. Ca^{2+} influx through VICCs has been suggested to be necessary to balance the Ca^{2+} efflux mechanisms and to participate in maintaining $[Ca^{2+}]c$ in unstimulated cells. Several Ca^{2+} channels located in the tonoplast (that is the vacuolar membrane) and ER are also described. They can be both voltage and ligand activated and mediate cytosolic Ca^{2+} rises.

Every kind of stress or developmental cue is thought to cause a typical cytosolic Ca^{2+} rise (called "Ca^{2+} signature") that, thanks to its spatial and temporal uniqueness, can in turn activate different proteins that function as effectors (White and Broadley, 2003).

6.2 H_2O_2 and Ca^{2+} signalling

Aerobic metabolic processes such as respiration and photosynthesis unavoidably led to the production of ROS in mitochondria, chloroplasts and peroxisomes. ROS can cause an oxidative damage to DNA, proteins and lipids, and so cells have evolved different systems that scavenge them. Plants are endowed with nonenzymatic and enzymatic scavenging mechanism. In the first class there are cellular redox buffers such as ascorbate, glutathione, flavonoids, carotenoids and others. The second class includes superoxide dismutase, ascorbate peroxidase, glutathione peroxidase and catalase. The first enzyme dismutates superoxide to H_2O_2, the other three detoxify H_2O_2 (Shao et al., 2008).

In the past few years emerging attention has been paid regarding the role of H_2O_2 in plant cells (Apel and Hirt, 2004). H_2O_2, being a small, diffusible and highly reactive molecule bears the fundamental properties of second messengers (Wang et al., 2008), and it is no longer considered only as a toxic molecule that plant cells must eliminate. Indeed numerous evidence has been obtained supporting the hypothesis that H_2O_2 functions as signalling molecule in plant cells (Apel and Hirth, 2004).

Moreover, a close correlation between H_2O_2 and Ca^{2+} has been reported: i) many stimuli, e.g. NaCl, induce both cytoplasmic Ca^{2+} increase and H_2O_2 production in plant cells (Leshem et al., 2007; Ranf et al., 2008); ii) Ca^{2+} and CaM *in vitro* can bind to, and activate, the plant peroxisomal Cat3, one of the three isoforms of the main H_2O_2 scavenging enzyme in eukaryotic cells, catalase (Yang and Poovaiah, 2002); iii) the HACCs identified in stomata guard and root cells are activated

by H_2O_2 (Demidchik et a., 2007); iv) Ca^{2+} directly stimulates the activity of plasma membrane proteins involved in H_2O_2 biosynthesis in response to biotic and abiotic stimuli (Apel and Hirt, 2004), the NADPH oxidases. All these data argue for a direct link between Ca^{2+}signalling and H_2O_2 production scavenging systems; however, despite the central role of these two second messengers in plant patho-physiology, a direct *in vivo* demonstration of this fact is still lacking.

The second part of this work started from these observations and was thus aimed at understanding if Ca^{2+} entry within plant peroxisomes can exert a role in such a fundamental function like control of H_2O_2 levels.

RESULTS

7.1 D3cpv-KVK-SKL targeting into plant peroxisomes

Plant and mammalian peroxisomes share similar protein import mechanism and peroxisomal targeting signals (Brown and Baker, 2008). In order to follow peroxisomal Ca^{2+} dynamics the cameleon probe D3cpv bearing the peroxisomal targeting signal KVK-SKL (Drago et al., 2008) was thus directly subcloned in a plant expression vector and expressed in tobacco cells. To confirm the proper peroxisomal localization of D3cpv-KVK-SKL an agroinfiltration experiment in tobacco leaves was performed: the Ca^{2+} probe was cotransformed with a peroxisomal marker, the Red Fluorescence Protein RFP-KSRM (Dammann et al., 2003). Figure 7.1a shows that the D3cpv-KVK-SKL signal detected, in transformed tobacco leaf cells, is localized in discrete structures with high motility (data not shown). The same structures were also detected when the leaf was imaged for the fluorescence of the RFP targeted to peroxisomes (Fig. 7.1 b). The overlay image (Fig. 7.1 c) clearly shows a perfect merge of the two signals (yellow) in the punctated structures, confirming the proper D3cpv-KVK-SKL peroxisome localization. It should be noted that agroinfiltration leads to independent cell transformation, hence the signal colocalization can occur only in cells coexpressing the two probes. The exclusive D3cpv-KVK-SKL peroxisome localization is supported also by the recognition of typical crystalline inclusions in the punctated fluorescent structures observed by means of fluorescence microscopy (data not shown) that are present in plant peroxisomes (Huang et al., 1983).

In order to perform an analysis of Ca^{2+} dynamics into the peroxisomal lumen of plant cells, stable *Arabidopsis* transgenic plants were generated with the 35S::D3cpv-KVK-SKL construct. Figures 7.1 d-e show the confocal analysis of a leaf from one of the selected transgenic *Arabidopsis* lines obtained (see Methods section, § 9). The signal is clearly localized in the peroxisomes of different cell types, such as epidermal, mesophyll and trichomes (Fig. 7.1 e, f) and no D3cpv-KVK-SKL mistargeting to other cellular structure was observed. Figures 1g-i show that D3cpv-KVK-SKL is expressed and properly localized also in *Arabidopsis* guard cell (Fig. 7.1 g, i).

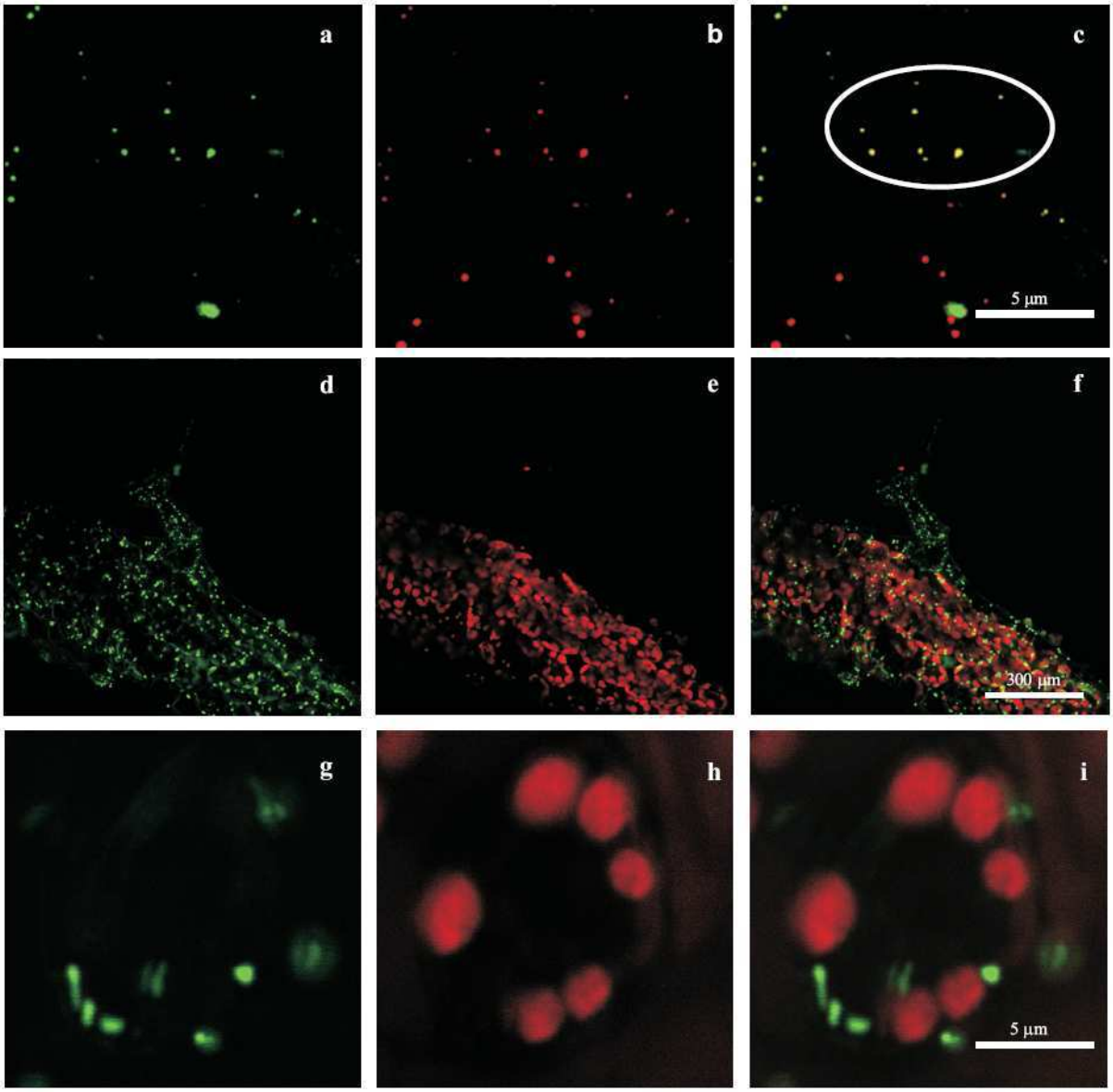

Figure 7.1. Subcellular distribution of D3cpv-KVK-SKL in transiently transformed tobacco epidermal cells and stable transgenic *Arabidopsis* Columbia plants. a-c. Confocal images of tobacco agroinfiltrated epidermal cells co-transformed with D3cpv-KVK-SKL and the peroxisomal marker RFP-KSRM. (a) Cameleon YFP fluorescence. b. RFP fluorescence. c. ovelay image of (a) and (b). d-i. Confocal images of stable transgenic *Arabidopsis* plants transformed with D3cpv-KVK-SKL. d. Cameleon YFP fluorescence in Arabidopsis leaf epidermal cells. e. chlorophyll fluorescence of the same leaf shown in (d). f. overlay image of (d) and (e). g. Cameleon YFP fluorescence in stomata guard cells. h. chlorophyll fluorescence of the same stomata guard cells shown in (g). i. overlay image of (g) and (h).

7.2 Ca^{2+} dynamics in peroxisomes of Arabidopsis guard cells

Two different groups (Drago et al., 2008; Lasorsa et al., 2008) have recently demonstrated in mammalian cell lines the existence of peroxisomal Ca^{2+} rises upon cellular stimulation. In order to investigate if this phenomenon occurs also in plant peroxisomes, experiments in *Arabidopsis* plants stably expressing D3cpv-KVK-SKL were performed. Guard cells were chosen as experimental model since there is a huge amount of data regarding conditions that can trigger a sustained cytoplasmic Ca^{2+} rise in this cell type (Allen et al., 2000; Yang et al., 2008). Among different stimuli one of the most reliable and easy to perform is the imposed membrane hyperpolarization. Figure 7.2 (black trace) shows Ca^{2+} imaging experiments performed in guard cells of *Arabidopsis* plants stably expressing the cytoplasmic GFP-based Ca^{2+} indicator YC3.60 (Nagai et al., 2001). As expected, cell hyperpolarization caused a sharp increase in the fluorescence emitted at 540 nm (YFP) and a decrease of the signal at 480 nm (CFP) and thus an increase in the 540/480 nm fluorescence emission ratio (Fig. 7.2, black trace), here presented as $\Delta R/R_0$, which is proportional to the $[Ca^{2+}]c$ (n=15). When the hyperpolarization was performed in the absence of external Ca^{2+}, no appreciable cytosolic $[Ca^{2+}]$ changes were observed (n=7), but the subsequent addition of 10 mM $CaCl_2$ induced a large Ca^{2+} increase (data not shown). After the initial and rapid increase cytosolic Ca^{2+} slowly returned toward basal level (Fig. 7.2). These results confirm previous data regarding Ca^{2+} dynamics in guard cells (Allen et al., 2000; Yang et al., 2008) and demonstrate that the cytosolic Ca^{2+} increase due to hyperpolarization is mainly, if not exclusively, due to Ca^{2+} entry from the extracellular space.

Figure 7.2 (grey trace) shows the typical response pattern of the D3cpv-KVK-SKL fluorescence (n=6) in guard cells of *Arabidopsis* plants stably expressing the probe. Notably, upon hyperpolarization also the peroxisomal $[Ca^{2+}]$ increased, but the maximum $\Delta R/R_0$ increase was reached more slowly within peroxisomes compared to the cytoplasm, similar to what already reported for peroxisomes in mammalian cells (Drago et al., 2008). When the hyperpolarization was performed without Ca^{2+} in the medium, no peroxisomal Ca^{2+} variations were observed (data not shown) (n=7).

The above results confirm and extend to plant cells the recent findings on peroxisome Ca^{2+} handling in animal cells by Drago et al., i.e. the $[Ca^{2+}]$ of these organelles essentially mimics the $[Ca^{2+}]$ of the cytoplasm, though the rate of peroxisome Ca^{2+} uptake is somewhat slower.

In order to obtain a rough estimate of the absolute peroxisomal $[Ca^{2+}]$ reached upon cellular stimulation, a calibration procedure similar to that used in mammalian cells (Drago et al. 2008) was used. The plasma membrane was permeabilized with digitonin, followed by passive Ca^{2+} loading

with different $CaCl_2$ concentrations. The data obtained suggest that during the hyperpolarization the peroxisomal [Ca^{2+}] is very similar to that in the cytosol (data not shown).

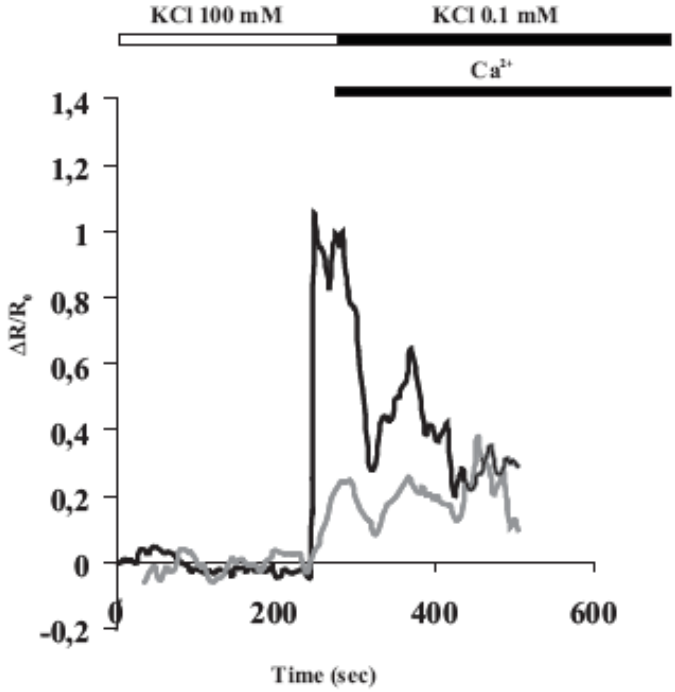

Figure 7.2. Cytoplasmic and intraperoxisomal Ca^{2+} monitoring in *Arabidopsis* guard cells subjected to plasma membrane hyperpolarization.

Cytoplasmic (black trace) and peroxisomal (grey trace) Ca^{2+} dynamics measurement with YC 3.60 and D3-KVK-SKL, respectively. Guard cells were bathed in depolarization buffer (white bar) and at the indicated time (250 sec) perfused with the hyperpolarization buffer (black bar) in presence of Ca^{2+}. Hyperpolarization induces a steep cytoplasmic Ca^{2+} rise temporally followed by an intraperoxisomal Ca^{2+} increase.

7.3 Targeting of a H_2O_2 sensor into cytoplasm and peroxisome of Arabidopsis plants

The question thus arises as to the physiological role of the peroxisomal [Ca^{2+}] changes. While no Ca^{2+} sensitive peroxisomal function is presently known in mammalian cells, in plant cells at least two key peroxisomal enzymes have been reported to be Ca^{2+} sensitive *in vitro* or in isolated peroxisomes: specifically, a catalase (Yang and Poovaiah, 2002) and a putative nitric-oxide synthase (Barroso et al., 1999). Peroxisome metabolism of H_2O_2 is of major importance in plant cells: not only peroxisome photorespiration has been demonstrated to produce massive amounts of H_2O_2 (50 times higher than that in the mitochondria) (Foyer and Noctor, 2003), but these organelles are the major site of H_2O_2 scavenging, due to the high concentration in their lumen of catalases (Nyathi and Baker, 2006). The ability of peroxisomal Ca^{2+} entry to affect H_2O_2 metabolism was thus investigated. To this end the new genetically encoded YFP-based H_2O_2 sensor HyPer was employed (Belousov et al., 2006). This probe has been so far successfully expressed in bacteria and animal cells where it was shown to be highly sensitive to H_2O_2 and not to be affected by other ROS. Stable transgenic *Arabidopsis* lines expressing the HyPer probe with two different subcellular localizations, cytoplasm and peroxisomes, were generated. In the case of peroxisomal HyPer the KSRM peptide, which constitute a PTS1 signal, was included at the protein C-terminal end (Fig. 7.3 top panel). In both cases the 2x35S promoter was used to direct the constitutive expression of the probes in all organs and tissues of the plant. Figures 7.3 a-d show confocal images of a representative *Arabidopsis* transgenic plant leaf expressing the cytoplasmic HyPer (cHyPer) that, as expected, presents a diffuse fluorescence, including a clear signal in the nucleus. Figures 7.3 e-h show confocal images of a representative *Arabidopsis* transgenic plant leaf expressing the HyPer-KSRM: in this latter case the fluorescence signal is localized in the typical small vesicular structures corresponding to the peroxisomes (Fig. 7.3 e-h). The peroxisomes of stomata guard cells were also strongly expressing the probes (Fig. 7.3 h).

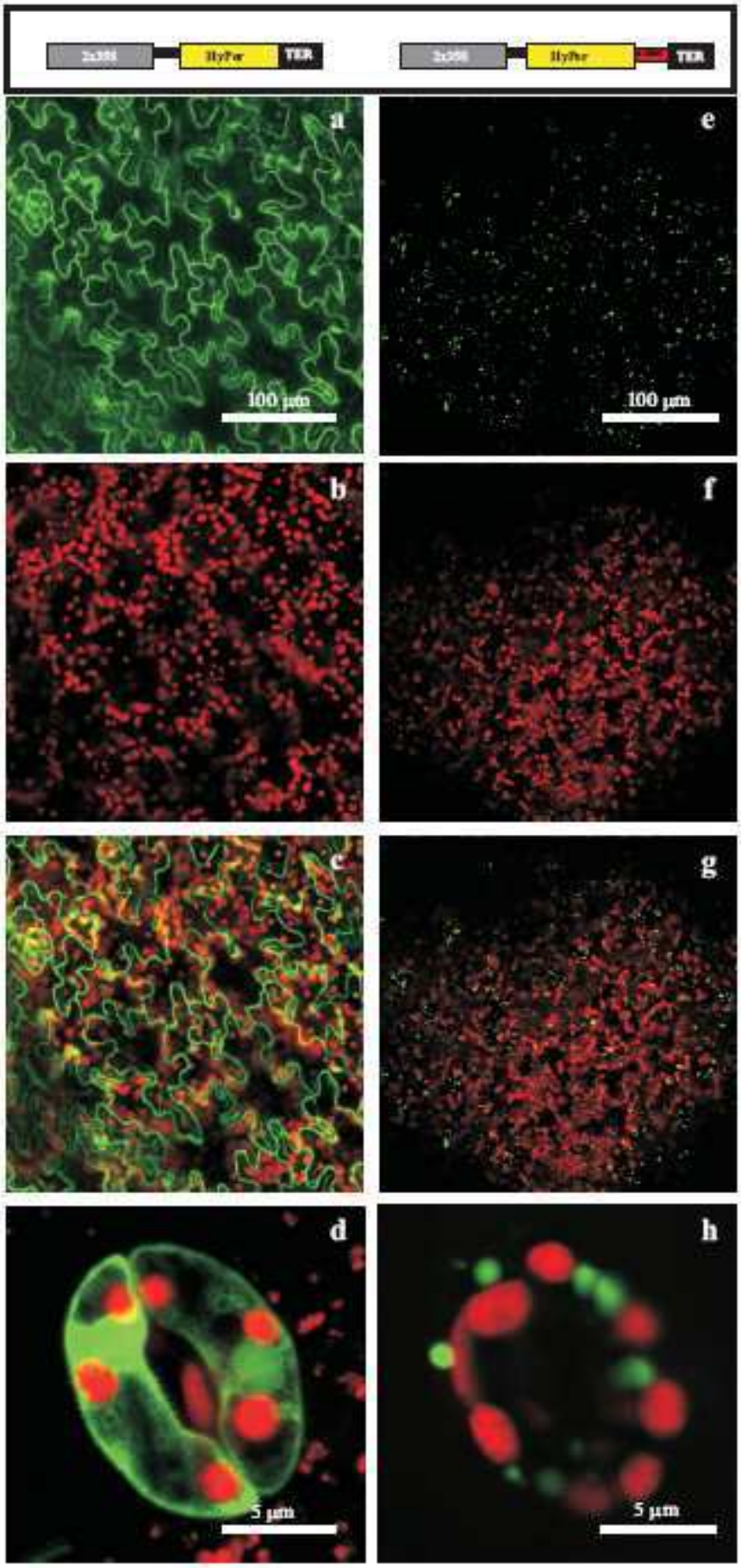
HyPer
TER
HyPer
TER
a
100 µm
e
100 µm
b
f
c
g
d
5 µm
h
5 µm

Figure 7.3. Subcellular distribution of HyPer and HyPer-KSRM in stable transgenic A*rabidopsis* plants. a-d. Confocal images of stable transgenic *Arabidopsis* plants transformed with cytoplasmic HyPer. a. HyPer fluorescence (green) in *Arabidopsis* epidermal leaf cells. b. chlorophyll fluorescence of the same leaf shown in (a). c. overlay image of (a) and (b). d. overlay image of HyPer (green) and chlorophyll (red) fluorescences in stomata guard cells. e-h. Confocal images of stable transgenic *Arabidopsis* plants transformed with HyPer-KSRM. e. HyPer fluorescence (green) in *Arabidopsis* leaf epidermal cells. f. chlorophyll fluorescence of the same leaf shown in (e). g. overlay image of (e) and (f). h. overlay image of HyPer (green) and chlorophyll (red) fluorescences in stomata guard cells.

7.4 H_2O_2 measurements in cytosol and peroxisomes of Arabidopsis guard cells

Arabidopsis plants expressing either cHyPer or HyPer-KSRM were used in order to follow H_2O_2 scavenging upon external H_2O_2 addition and to investigate if this phenomenon is affected by cellular Ca^{2+} rises.

Addition of 100 μM H_2O_2 to cHyPer expressing guard cells induced a sharp increase in the fluorescence intensity (emission 530 nm) when the probe was excited at 480 nm and a decrease of fluorescence when excited at 420 nm. The excitation ratio increase, here presented as $\Delta R/R_0$, was proportional to the amount of H_2O_2 added to the medium.

In guard cells expressing peroxisome localized HyPer, the fluorescence excitation ratio increased sharply upon addition of H_2O_2 with a $\Delta R/R_0$ peak average corresponding to 0.75 ± 0.237 (n=15) followed by a slight decrease and then by a sustained phase (Fig. 7.4). When cells were hyperpolarized after adding H_2O_2, (Fig. 7.4, grey trace) no significant difference was observed. However, when Ca^{2+} was added during the hyperpolarization protocol in order to cause a sustained Ca^{2+} entry, a fast acceleration of the fluorescence decay was observed (n=10). Similarly, when Ca^{2+} was present in the bath solution from the beginning of the hyperpolarization, the addition of H_2O_2 caused the usual $\Delta R/R_0$, but a fast fluorescence decrease was initiated upon hyperpolarization (Fig. 7.4, black trace) (n=15). Addition of Ca^{2+} was able to efficiently increase the HyPer fluorescence drop even when 1 mM H_2O_2 was used (data not shown).

The experiments presented in Fig. 7.4 were then repeated in guard cells expressing cHyPer. Also in this case the hyperpolarizing protocol, when carried out in the absence of Ca^{2+}, resulted in no significant alteration in the H_2O_2 levels, while a rapid decrease in cHyPer fluorescence occurred when Ca^{2+} was included in the hyperpolarizing medium (data not shown).

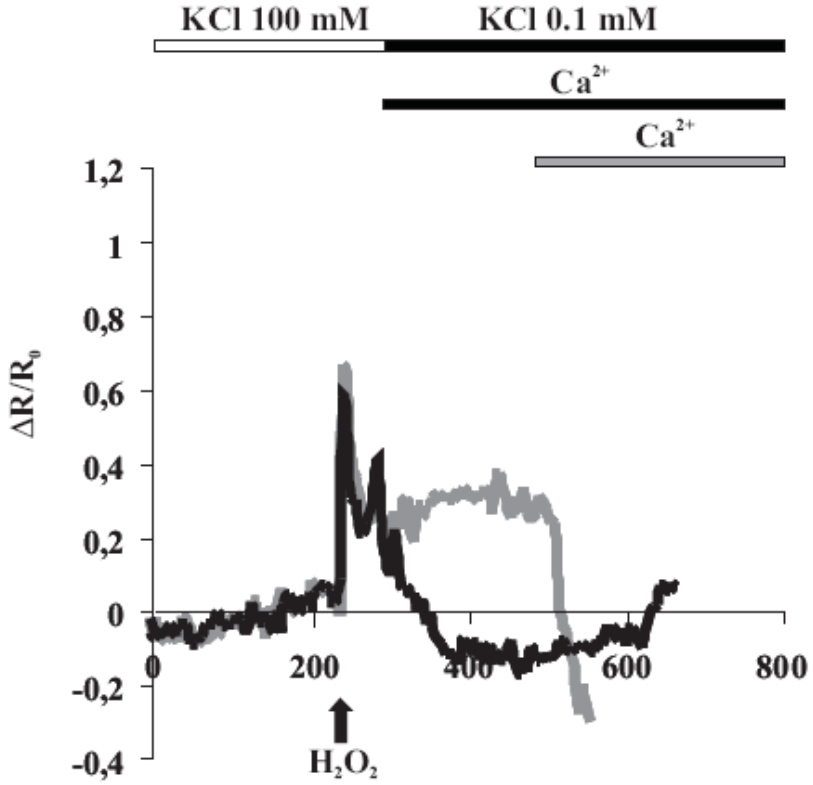

Figure 7.4. Ca^{2+} dependent peroxisomal H_2O_2 scavenging in *Arabidopsis* guard cells. *Arabidopsis* guard cells were bathed in depolarization buffer and at 250 sec 100 mM H_2O_2 was added (black arrow). The H_2O_2addition induced an immediate increase in the HyPer fluorescence (expressed as $\Delta R/R_0$) that was followed by a steep decrease (black trace) when cells were perfused (300 sec) with the hyperpolarization solution in presence of external Ca^{2+}. Interestingly, when plasma membrane hyperpolarization was carried out in absence of external Ca^{2+} the fast HyPer fluorescence drop was not observed (grey trace). The following Ca^{2+} addition (500 sec) induced a steep decrease in the HyPer fluorescence.

The simplest explanation of the data presented above is that the rise of Ca^{2+} induced by hyperpolarization results in the activation of the catalase isoform, Cat3, which is highly expressed in plant peroxisomes and is known to be activated by Ca^{2+} and CaM *in vitro* (Yang and Poovaiah, 2002). However, the possibility that the effect on HyPer fluorescence was due to effects other than Cat3 activation should be considered. In particular, the possibility that cytosolic or peroxisome pH change should be excluded, as pH acidification causes a $\Delta R/R_0$. In the original HyPer work Belousov and colleagues (Belousov et al., 2006) reported that pH can affect the HyPer fluorescence similarly to other GFP based sensors such as Pericam (Nagai et al., 2001). Indeed when *Arabidopsis* guard cells expressing the HyPer-KSRM were challenged with NH_4Cl or NaAc, to induce alkalinization or acidification of both cytoplasm and organelles pH major changes of the $\Delta R/R_0$

were observed. Figure 7.5 shows that addition of 1 mM NH_4Cl determines a slow increase of $\Delta R/R_0$, while 5 mM NaAc caused a sharp fluorescence decrease (n=6). Notably, however, the increase in $\Delta R/R_0$ of HyPer, as induced by NH_4Cl, was not affected by Ca^{2+} entry (n=6). Moreover, HyPer is still able to sense H_2O_2, as demonstrated by the peak following H_2O_2 addition. Similar results were obtained with cHyPer.

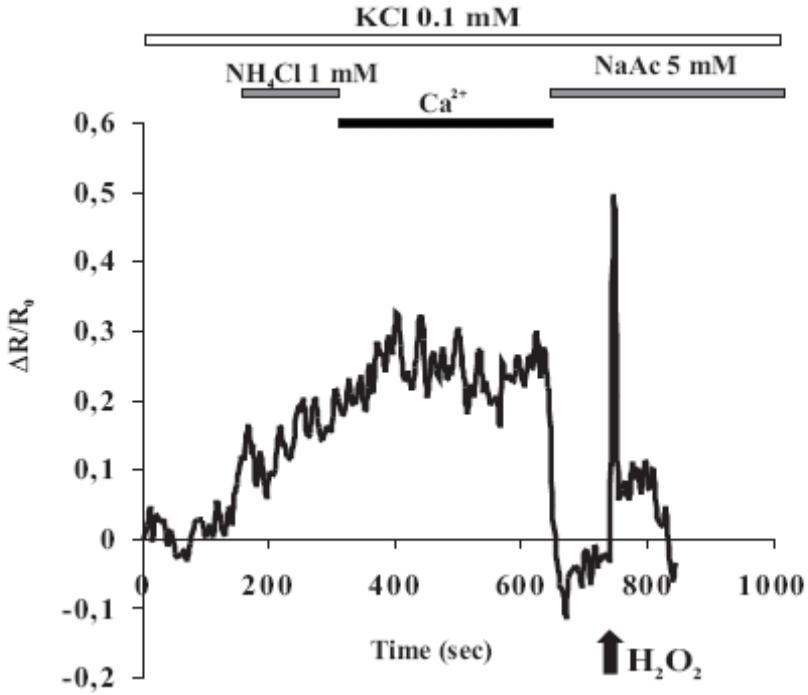

Figure 7.5. The Ca^{2+}- dependent HyPer fluorescent drop is strictly dependent on the H_2O_2 removal and is not affected by pH changes. *Arabidopsis* guard cells were bathed in hyperpolarization buffer and at 150 sec 1 mM of NH_4Cl was added. The NH_4Cl mediated cytoplasmic alkalinization induced a slow rise of HyPer fluorescence in peroxisomes. The signal was not affected by the following Ca^{2+} entry. The cytoplasmic acidification mediated by 5 mM NaAc administration (600 sec) induced a drop in the HyPer fluorescence that was recovered by 100 mM H_2O_2 addition resulting in a typical sharp and fast HyPer fluorescence increase.

8. DISCUSSION

Based on the recent demonstration that mammalian peroxisomes can participate in cellular Ca^{2+} homeostasis, experiments in plant peroxisomes were carried out in order to investigate if this phenomenon occurs also in plants and if it can regulate some physiological functions. The probe D3cpv-KVK-SKL was targeted into plant peroxisomes by a simple subcloning of its cDNA in a plant expression vector. As expected from the similar mammalian and plant peroxisomal protein import mechanism, the probe was correctly targeted into peroxisomes: this is demonstrated by the colocalization with a peroxisomal marker (RFP-KSRM), but also by the high motility of the organelles and from the presence of crystalline inclusion, two features of plant peroxisomes that allow their easy identification. Notably, while in mammalian peroxisomes a small percentage of cell expressing D3cpv-KVK-SKL shows a mistargeting to the cytosol of the probe, in plant cells this phenomenon was never observed.

Ca^{2+} measurements in mammalian peroxisomes with D3cpv-KVK-SKL demonstrated that peroxisomes slowly equilibrate with $[Ca^{2+}]c$. Guard cells were chosen as the experimental model, since they are the plant cell type best characterized concerning Ca^{2+} signalling. One of the best ways to cause a strong and reproducible cytosolic Ca^{2+} elevation in guard cells is shifting the bathing medium from a high to a low KCl containing in the presence of Ca^{2+}. As expected, this treatment caused a Ca^{2+} rise in cytosol and also in peroxisomes, in the latter with a slower kinetic, if compared to the cytosol. The process is mainly due to Ca^{2+} entry from outside the cell, since hyperpolarization in a medium devoid of Ca^{2+} failed to cause a Ca^{2+} rise in either compartment.

The question about a physiological role of peroxisomal Ca^{2+} entry was then addressed starting from the *in vitro* demonstration that a peroxisomal plant catalase isoform is CaM-Ca^{2+} regulated (Yang and Poovaiah, 2002). Experiments in order to understand if H_2O_2 scavenging is somehow influenced by Ca^{2+} rises were thus performed. A new H_2O_2 sensor called HyPer was stably expressed in plant cytosol or peroxisomes and it revealed the existence of a Ca^{2+}-dependent H_2O_2 scavenging. This phenomenon is Ca^{2+} dependent, since hyperpolarization without Ca^{2+} in the external bathing solution didn't cause a fast drop in H_2O_2 level. The possibility that HyPer emission drop is caused by something else than activation of a Ca^{2+}-dependent scavenging system was also considered. In particular, the possibility that the drop is caused by a cytosolic acidification was excluded, since H_2O_2 treatment or depolarization cause, if any, only minor changes in intracellular pH.

A strong molecular candidate for this Ca^{2+}-activated H_2O_2 scavenging is Cat3, since it has been reported to be Ca^{2+}-CaM activated. However, a direct *in vivo* evidence supporting this hypothesis is still missing. At the time of writing, experiments aimed at directly proving this hypothesis are being carried out. They are based on two different approach: i) overexpression and silencing of Cat3 by agroinfiltration experiments in tobacco plants with the cDNA coding for Cat3 or its antisense in coexpression with the HyPer-KSRM probe; ii) recently an age-dependent Cat3 expression was demonstrated (Du et al., 2008); a rise in Ca^{2+} activated H_2O_2 scavenging in HyPer-expressing *Arabidopsis* plants is thus expected in older plants. Preliminary results confirm the hypothesis that Cat3 is responsible for the Ca^{2+}-activated H_2O_2 scavenging observed.

9. METHODS

Plant material and growth condition. All the *Arabidopsis thaliana* plants were of the Columbia ecotype. Plants were grown in soil under 16/8 h cycles of light (70 mmol m-2 sec-1) at 20 °C. The transgenic pGC1-YC3.60 *Arabidopsis* plants were generated and reported for a previous study (Yang et al., 2008).

DNA constructs. The RFP-KSRM construct was digested from the pRTL2 vector by PstI digestion and ligated in the pGreen0029 binary vector (Hellens et al., 2000).
The D3cpv-KVK-SKL construct was digested from the pcDNA3 vector with HindIII and EcoRI and ligated in the 35S-CaMV cassette vector (http://www.pgreen.ac.uk/JIT/JIT_fr.htm). The entire cassette was then partially digested with EcoRV and ligated in the pGreen0179 binary vector.
The HyPer cDNA was amplified by PCR by using the Phusion® DNA Polymerase (Finnzymes, Finland) from the purchased pHyPer-Cyto vector (http://www.evrogen.com/products/HyPer/HyPer.shtml, Evrogen, Russia). For both the cytoplasmic and peroxisomal localization of HyPer the same forward primer was used: 5'-CATGCCATGGAGATGGCAAGCCAGCA-3'. An NcoI restriction site was introduced at the 5' end. The 3' reverse primer for the subcloning of the cytoplasmic localized HyPer was: 5'-TGGAAGATCTTTAAACCGCCTGTTTTAAAACT-3', for the peroxisomes localization the KSRM peptide coding sequence was inserted upstream of the HyPer stop codon 5'-TGGAAGATCTCACATCCTGGATTTAACCGCCTGTTTTAAA-3'. In both cases a BglII restriction site was introduced. The amplicons were then digested and inserted in the pAVA554 vector (von Arnim et al., 1998) downstream of the double 35S promoter and the translational enhancer sequence of TEV. The obtained vectors were sequenced to verify that no mistakes were introduced by PCR amplification. The entire expression cassettes of both cHyPer and HyPer-KSRM were thereafter isolated from the pAVA554 modified vectors by digestion with KpnI/SacI and ligated in the pGreen 0179 binary vector. All the pGreen binary vectors obtained were introduced in the *Agrobacterium tumefaciens* GV3101 strain harbouring the pSoup helper plasmid.

Transgenic plants. The *Agrobacterium* strains obtained were used for both tobacco agroinfiltration experiments or to generate transgenic *Arabidopsis* plants by floral-dip method. For each construct different *Arabidopsis* independent transgenic lines were selected and for imaging experiments two

independent lines were employed. No one of the transgenic lines obtained with the different constructs showed phenotypic differences or abnormalities in our standard growth conditions.

Confocal microscopy analyses. Confocal microscopy analyses were performed using a Nikon PCM2000 (Bio-Rad, Germany) laser scanning confocal imaging system. For Cameleon-dependent YFP and HyPer detection, excitation was at 488 nm and emission between 530/560 nm. For the chlorophyll detection, excitation was at 488 nm and detection over 600 nm. For RFP detection, excitation was set at 548 nm and emission 573 nm. Image analysis was done with the ImageJ bundle software (http://rsb.info.nih.gov/ij/).

Guard Cell Imaging. For guard cell imaging leaves of 4-5 weeks-old *Arabidopsis* plants were attached to microscope cover glasses using a Medical adhesive (Hollister Inc., Libertyville, IL). A paintbrush was used to gently press the leaf to the coverslip and upper cell layers were carefully removed using a razor blade. Cells expressing the fluorescent probes were analyzed using an inverted fluorescence microscope (Zeiss Axioplan) with an immersion oil objective (X63, N.A. 1.40, for fluorescent probes). Excitation light was produced by a monochromator (Polychrome II; TILL Photonics, Martinsried, Germany). For Hyper probe, excitation lights were 420 and 480 nm. The two excitation wavelengths were rapidly alternated and the emitted light deflected by a dichroic mirror (455DRPL) was collected through emission filters (480 ELFP). For theYC3.60 and D3cpv-KVK-SKL probes, the excitation light was 425 nm. The emitted light was collected through a beamsplitter (OES s.r.l., Padua, Italy) (emission filters HQ480/40M for cyan fluorescent protein and HQ 535/30M for yellow fluorescent protein) and a dichroic mirror (515 DCXR). Filters and dichroic mirrors were purchased from Omega Optical and Chroma. Images were acquired using a cooled CCD camera (Imago; TILL Photonics) attached to a 12-bit frame grabber. Synchronization of the monochromator and CCD camera was performed through a control unit run by TILLvisION v.4.0 (TILL Photonics); this software was also used for image analysis. For time course experiments, the fluorescence intensity was determined over regions of interests corresponding to an entire guard cell for cHyPer and YC3.60 or covering small groups of peroxisomes expressing HyPer-KSRM or D3cpv-KVK-SKL. Exposure time and frequency of image capture varied from 100 to 500 ms and from 5 to 0.2 Hz, respectively. Cells were mounted into an open-topped chamber and maintained in the depolarization (100 mM KCl, 0.5 mM EGTA and 10 mM Mes-Tris pH 6.15) or hyperpolarization (0.1 mM KCl, 0.5 mM EGTA and 10 mM Mes-Tris pH 6.15) buffers. For the Ca^{2+} addition the hyperpolarization buffer was prepared as follow: 0.1 mM KCl, 10 mM $CaCl_2$, 0.5 mM EGTA and 10 mM Mes-Tris pH 6.15.

Plasma membrane permeabilization was performed by treating cells for 2 min with 1 mM digitonin in an intracellular-like medium containing (in mM): 100 potassium-gluconate, 1 $MgCl_2$, 10 Hepes, pH 7.5, at and 0.5 EGTA. Experiments with permeabilized cells were performed in the same medium; where indicated, the latter was supplemented with the same buffer containing 2 mM $CaCl_2$.

10. REFERENCE LYST

- Allen, G. Chu, S.P., Schumacher, K., Shimazaki, C.T., Vafeados, D., Kemper, A., Hawke, S.D., Tallman, G., Tsien, R.Y., Harper, J.F., Chory, J. and Schroeder, J.I. (2000). Alteration of stimulus-specific guard cell calcium oscillations and stomatal closing in Arabidopsis det3 mutant. Science. 289, 2338-2342.
- Apel, K. and Hirt, H.(2004) Reactive oxygen species: metabolism, oxidative stress, and signal transduction. Annu Rev Plant Biol. 55, 373-99.
- Baird, G.S., Zacharias, D.A. and Tsien, R.Y. (1999). Circular permutation and receptor insertion within green fluorescent proteins. Proc. Natl. Acad. Sci. USA 96, 11241-11246.
- Barroso, J.B., Corpas, F.J., Carreras, A., Sandalio, L.M., Valderrama, R., Palma, J.M., Lupiáñez, J.A. and del Río, L.A. (1999). Localization of nitric-oxide synthase in plant peroxisomes. J Biol Chem. 274, 36729-36733.
- Belousov, V.V., Fradkov, A.F., Lukyanov, K.A., Staroverov, D.B., Shakhbazov, K.S., Terskikh, A.V. and Lukyanov, S. (2006). Genetically encoded fluorescent indicator for intracellular hydrogen peroxide. Nat Methods 3, 1-286.
- Berridge, M. J., Bootman, M. D. e Roderick, H.L. (2003). Ca^{2+}-signalling: dynamics, homeostasis and remodelling. Nat. Rev. Mol. Cell. Bio. 4, 517-29.
- Braverman, N., Steel, G., Obie, C., Moser, A., Moser, H., Gould, S.J. and Valle, D. (1997). Human PEX7 encodes the peroxisomal PTS2 receptor and is responsible for rhizomelic chondrodysplasia punctata. Nat Genet. 15, 369-76.
- Brown, L. and Baker, A. (2008). Shuttles and cycles: transport of proteins into the peroxisome matrix. Molecular Membrane biology 25 (5), 363-375.
- Camoes, F., Bonekamp, N.A., Delille, H. K. and Shraeder M. (2008). Organelle dynamics and dysfunction: a closer link between peroxisomes and mitochondria. J inherit Metab Dis.
- Carafoli, E. (2005). Calcium- a universal carrier of biological signals. FEBS J. 272, 1073-1089.
- Catterall, W.A. and Few, A.P. (2008). Calcium channel regulation and synaptic activity. Neuron. 59, 882-901.
- Clapham D. (2007) Calcium signalling. Cell 131, 1047-1058.
- Csordas, G., Thomas, A.P. and Hajnoczky, G. (1999). Quasi-synaptic calcium signal transmission between endoplasmic reticulum and mitochondria. EMBO J. 18, 96-108.
- Dammann, C., Ichida, A., Hong, B., Romanowsky, S.M., Hrabak, E.M., Harmon, A.C., Pickard, B.G. and Harper, J.F. (2003). Subcellular targeting of nine calcium-dependent protein kinases isoforms from *Arabidopsis*. Plant physiol. 132, 1840-1848.

- Dansen, T., Wirtz, K., Wanders, R. and Pap, E. (2000). Peroxisome in human fibroblast have a basic pH. Nat. Cell. Biol. 2, 51-53.
- DeBrito, O.M. and Scorrano, L. (2008). Mitofusin 2 tethers endoplasmatic reticulum to mitochondria. Nature. 456, 605-610.
- Demidchik, V., Shabala, S.N. and Davies, J.M. (2007). Spatial variation in H_2O_2 response of *Arabidopsis* thaliana root epidermal Ca^{2+} flux and plasma membrane Ca^{2+} channels. Plant J. 49, 377-386.
- Donato, R. (1999). Functional roles of S100 proteins, calcium-binding proteins of the EF-hand type. BBA. 1450, 199-231.
- Drago, I., Giacomello, M., Pizzo, P. and Pozzan, T. (2008). Calcium dynamics in the peroxisomal lumen of living cells. J Biol Chem. 283, 14384-14390.
- Du, Y., Wang P., Chen, J. and Song, C. (2008). Comprehensive Functional Analysis of the Catalase Gene Family in Arabidopsis thaliana. J of Integr Plant Biol. 50, 1318-1326.
- Haug-Collet, K., Pearson, B., Webel, R., Szerencsei, R.T., Winkfein, R.J., Schnetkamp, P.P. and Colley, NJ. (1999). Cloning and characterization of a potassium-dependent sodium/calcium exchanger in Drosophila. J Cell Biol 147, 659–670.
- Huang, A.H.C., Trelease, R.N. and Moore, T.S. (1983). Plant Peroxisomes. Academic Press
- Hoepfner, D., Schildknegt, D., Braakman, I., Philippsen, P. and Tabak, H. F. (2005).Contribution of the endoplasmic reticulum to peroxisome formation. Cell 122, 85-95.
- Fasolato, C., Innocenti B. and Pozzan T. (1994). Receptor-activated Ca^{2+} influx: how many mechanisms for how many channels? Trends Pharmacol. Sci. 15, 77-82.
- Filippin, L., Magalhães, P.J., Di Benedetto, G., Coltella, M. and Pozzan, T. (2003). Stable interactions between mitochondria and endoplasmic reticulum allow rapid accumulation of calcium in a subpopulation of mitochondria. J Biol Chem. 378, 39224- 34.
- Foyer, C.H. and Noctor, G. (2003). Redox sensing and signalling associated with reactive oxygen in chloroplasts, peroxisomes and mitochondria. Physiol. Plant. 119, 355-364.
- Fujiki, Y., Okumoto, K., Kinoshita, N. and Ghaedi, K. (2006). Lessons from peroxisome-deficient Chinese hamster ovary cell mutants. Biochem Biophys Acta. 1763, 1374-81.
- Giacomello, M., Drago, I., Pizzo, P. and Pozzan, T. (2007). Mitochondrial Ca^{2+} as a key regulator in cell life and death. Cell death diff. 14, 1267-1274.
- Griesbeck, O., Baird, G.S., Campbell, R.E., Zacharias, D.A. and Tsien, R.Y. (2001). Reducing the environmental sensitivity of yellow fluorescent protein. Mechanism and applications. J. Biol. Chem. 276, 29188–29194.

- Hellens, R.P, Edwards, E.A., Leyland N,R., Bean, S. and Mullineaux, P.M. (2000). pGreen: a versatile and flexible binary Ti vector for Agrobacterium-mediated plant transformation. Plant Mol. Biol. 42, 819-832.
- Hoeflich, K.P. and Ikura, N. (2002). Calmodulin in action: diversity in target recognition and activation mechanisms. Cell. 108, 739-742.
- Hoepfner, D., Schildknegt, D., Braakman, I., Philippsen, P. and Tabak, H.F. (2005) Contribution of the endoplasmic reticulum to peroxisome formation. Cell. 122, 85-95.
- Hutton, D. and Steinberg, D. (1973). Localization of the enzymatic defect in phytanic acid storage disease (Refsum's disease). Neurology. 23, 1333-4.
- Jankowski, A., Kim, J., Collins, R., Daneman, R., Walton, P. and Grinstein, S. (2001). In Situ Measurements of the pH of Mammalian Peroxisomes Using the Fluorescent Protein pHluorin. J. Biol. Chem. 276, 48748- 48763.
- Kliewer, S.A., Umesono, K., Noonan, D.J., Heyman, R.A. and Evans, R.M. (1992). Convergence of 9-cis retinoic acid and peroxisome proliferator signalling pathways through heterodimer formation of their receptors. Nature. 358, 771-774.
- Lasorsa, F.M., Scarcia, P., Erdmann, R., Calmieri, F., Rottensteiner, H., Calmieri, L. (2004). The yeast peroxisomal adenine nucleotide transporter: characterization of two transport modes and involvement in DeltapH formation across peroxisomal membranes.J Biol Chem. 381, 581-585.
- Lasorsa, F.M., Pinton, P., Palmieri, L., Scarcia, P., Rottensteiner, R., Rizzuto, R. and Palmieri, F. (2008). Peroxisomes as novel players in cellular Ca^{2+} homeostasis. J. Biol. Chem. 283, 15300-8.
- Leshem, Y., Seri, L. and Levine, A. (2007). Induction of phosphatidylinositol 3-kinase-mediated endocytosis by salt stress leads to intracellular production of reactive oxygen species and salt tolerance. Plant J. 51, 185-197.
- Leon, S., Goodman, J. and Subramani S. (2006). Uniqueness of the mechanism of protein import into the peroxisome matrix: ttransport of folded, co-factor boun and oligomeric proteins by shuttling receptors. BBA 1763 1552-1564.
- Matsuzaki, T. and Fujiki, Y. (2008). The peroxisomal membrane protein import receptor Pex3p is directly transported to peroxisomes by a novel Pex19p- and Pex16p-dependent pathway. J Cell Biology.183, 1275-86.
- Minta, A., Kao, J.P. and Tsien, R.Y. (1989). Fluorescent indicators for cytosolic calcium based on rhodamine and fluorescein chromophores. J Biol Chem .264, 8171-8178.

- Miyawaki, A. (2005). Innovations in the imaging of brain functions using fluorescence probes. Neuron. 48, 189-199.
- Miyawaki, A., Griesbeck, O., Heim, R. and Tsien, R.Y. (1999). Dynamic and quantitative Ca^{2+} measurements using improved cameleons. Proc. Natl. Acad. Sci. USA 96, 2135-2140.
- Miyawaki, A., Llopis, J., Heim, R., McCaffery, J.M., Adams, J.A., Ikura, M. and Tsien, R.Y. (1997). Fluorescent indicators for Ca^{2+} based on green fluorescent proteins and calmodulin. Nature 388, 882-887.
- Mosser J., Douar, A.M., Sarde, C.O., Kioschis, P., Feil, R., Moser, H., Poustka, A.M., Mandel, J.L. and Aubourg, P. (1993). Putative X-linked adrenoleukodystrophy gene shares unexpected homology with ABC transporters. Nature. 25, 26-30.
- Nagai, T., Ibata, K., Park, E.S., Kubota, M., Mikoshiba, K. and Miyawaki, A. (2002). A variant of yellow fluorescent protein with fast and efficient maturation for the cell application. Nature Biotechnol. 20, 87-90.
- Nagai, T., Sawano, A., Park, E.S. and Miyawaki, A. (2001). Circularly permutated green fluorescent proteins engineered to sense Ca^{2+}. Proc. Natl. Acad. Sci. USA 98, 3197-3202.
- Neuberger, G., Maurer-Stroh, S., Eisenhaber, B., Hartig, A. and Eisenhaber, F. (2003). Prediction of peroxisomal targeting signal 1 containing proteins from amino acid sequence. J Mol Biol. 328, 581-92.
- Neuspiel, M., Schauss, A., Braschi, E., Zunino, R., Rippstein, P., Rachubinski, R., Andrade-Navarro M. and McBride, H. (2008). Cargo-selected transport from the mitochondria to peroxisomes is mediated by vesicular carriers. Curr. Biol. 18, 102-108.
- Nito, K., Kamigaki, A., Kondo, M., Hayashi, M. and Nishimura, M. (2007). Functional classification of Arabidopsis peroxisome biogenesis factors proposed from analyses of knockdown mutants. Plant Cell Physiol. 48, 763-74.
- Nyathi, Y. and Baker, A. (2006). Plant peroxisomes as a source of signalling molecules. Biochim Biophys Acta 1763, 1478-1495.
- Oliveira, M.E., Gouveia, A.M., Pinto, R.A., Sá-Miranda, C. and Azevedo, J.E. (2003). The energetics of Pex5p-mediated peroxisomal protein import. J Biol Chem. 278, 39483-8.
- Palmer, A., Giacomello, M., Kortemme, T., Hires, A., Lev-Ram, V., Baker, D., and Tsien, R.Y. (2006). Ca^{2+} Indicators Based on Computationally Redesigned Calmodulin-Peptide Pairs. Chemistry & Biology 13, 521–530.
- Pei, Z.M., Murata, Y., Benning, G., Thomine, S., Klüsener, B., Allen, G.J., Grill, E. and Schroeder, J.I. (2000). Calcium channels activated by hydrogen peroxide mediate abscisic acid signalling in guard cells. Nature. 406, 731-4

- Pietrobon, D., Di Virgilio, F. and Pozzan, T. (1990). Structural and functional aspects of calcium homeostasis in eukaryotic cells. Eur. J. Biochem. 193, 599-622
- Pinton, P., Pozzan, T. and Rizzuto, R. (1998). The Golgi apparatus is an inositol 1,4,5-trisphosphate-sensitive Ca^{2+} store, with functional properties distinct from those of the endoplasmic reticulum. EMBO J. 18, 5298-5308
- Platta, H. and Erdmann, R. (2007). Peroxisomal dynamics. Trends in cell biol. 17, 474- 484.
- Pozzan T., Magalhaes, P. and Rizzuto, R. (2000). The comeback of mitochondria to calcium signalling. Cell Calcium. 28, 279–283.
- Pozzan, T., Rizzuto, R., Volpe, P. and Meldolesi, J. (1994). Molecular and cellular physiology of intracellular calcium stores. Physiol. Rev. 74, 595-636.
- Prasher, D., McCann, R.O. and Cormier, M.J. (1985). Cloning and expression of the cDNA coding for aequorin, a bioluminescent calcium-binding protein. Biochem. Biophys. Res. Commun. 126, 1259-68.
- Ranf, S., Wünnenberg P., Lee J., Becker D., Dunkel M., Hedrich R., Scheel D. and Dietrich P. (2008). Loss of the vacuolar cation channel, AtTPC1, does not impair Ca^{2+} signals induced by abiotic and biotic stresses. Plant J. 53, 287-299.
- Rizzuto, R., Brini, M., Murgia, M. and Pozzan, T. (1993). Microdomains with high Ca^{2+} close to IP_3-sensitive channels that are sensed by neighboring mitochondria. Science 262, 744-747.
- Rizzuto, R., Pinton, P., Carrington, W., Fay, F. S., Fogarty, K. E., Lifshitz, L. M., Tuft, R. A., and Pozzan, T. (1998). Close contacts with the endoplasmic reticulum as determinants of mitochondrial Ca^{2+} responses. Science 280, 1763-1766.
- Rizzuto, R. and Pozzan, T. (2006). Microdomains of Intracellular Ca^{2+}: Molecular Determinants and Functional Consequences. Physiol Rew. 86, 369-408.
- Rizzuto, R., Simpson, A.W.M., Brini, M. and Pozzan, T. (1992). Rapid changes of mitochondrial Ca^{2+} revealed by specifically targeted recombinant aequorin. Nature 358, 325-327.
- Roberts, S. and Snowman, B. (2000). The effects of ABA on channel-mediated K(+) transport across higher plant roots. J Exp Bot. 51, 1585-1594.
- Rudolf R., Mongillo M., Rizzuto, R. and Pozzan, T. (2003). Looking forward to seeing calcium. Nat. Rev. Mol. Cell. Bio. 4, 579-586.
- Santos, M.J., Imanaka, T., Shio, H., Small, G.M. and Lazarow, P.B. (1998). Peroxisomal membrane ghosts in Zellweger syndrome--aberrant organelle assembly. Science. 239, 1536-8.
- Shaner, N., Patterson, G.H. and Davidson, M.W. (2007). Advances in fluorescent protein technology. J Cell Sci. 120, 4247- 4260.

- Shao, H.B., Chu, L.Y., Shao, M.A., Jaleel, C.A. and Mi, H.M. (2008). Higher plant antioxidants and redox signalling under environmental stresses. C R Biol. 6, 433-41.
- Shimomura, O., Johnson, F.H. and Saiga, Y. (1962). Extraction, purification and properties of aequorin, a bioluminescent protein from the luminous hydromedusan Aequorea. Biochemistry 13, 2656-2662.
- Shrader, M. and Fahimi, H.D. (2006). Peroxisomes and oxidative stress. BBA. 1763, 1755-1766.
- Shrader, M. and Fahimi, H.D. (2008). The peroxisome: still a mysterious organelle. Histochem Cell Biol. 129, 421-40.
- Steinberg, S., Dodt, G., Raymond, G., Braverman, N., Moser, A. and Moser, H. (2006). Peroxisome biogenesis disorders. BBA. 1763, 1733-1748.
- Titorenko, V.I., Nicaud J., Wang H., Chan H. and Rachubinski R.A. (2002). Acyl-CoA oxidase is imported as a heteropentameric, cofactor-containing complex into peroxisomes of Yarrowia lipolytica. Journal of Cell Biol. 156, 481-494.
- Titorenko, V. and Rachubinski, R. (2004). The peroxisome: orchestrating important developmental decisions from inside the cell. J Cell biol. 164, 641-645.
- Titorenko, V. I., Ogrydziak, D. M. and Rachubinski, R. A. (1997). Four distinct secretory pathways serve protein secretion, cell surface growth, and peroxisome biogenesis in the yeast Yarrowia lipolytica. Mol. Cell. Biol. 17, 5210-5226.
- Tsien, R. Y. (1980) New calcium indicators and buffers with high selectivity against magnesium and protons: design, synthesis, and properties of prototype structures. Biochemistry 19, 2396–2404
- Tsien, R.Y. (1998). The green fluorescent protein. Annu. Rev. Biochem. 67, 509-544.
- Van der Zand, A., Braadkman, I., Geuze, H. and Tabak, F. (2006) The return of the peroxisome. J. Cell Sci. 119 989-994.
- van Roermund, C.W., de Jong, M., IJlst, L., van Marle, J., Dansen, T.B., Wanders, R.J. and Waterham, H.R. (2004). The peroxisomal lumen in Saccharomyces cerevisiae is alkaline. J Cell Sci. 117, 4231-7.
- Völkl, A., Mohr, H. and Fahimi, H.D.(1999). Peroxisome subpopulations of the rat liver. Isolation by immune free flow electrophoresis. J Histochem Cytochem. 47, 1111-8.
- von Arnim, A.G., Deng, X.W. and Stacey, M.G. (1999). Cloning vectors for the expression of green fluorescent protein fusion proteins in transgenic plants. Gene. 221, 35-43.
- Wanders, R. and Waterham, H. (2006). Biochemistry of mammalian peroxisome revisited. Annu. Rev. Biochem. 75, 295-332.

- Wanders, R. and Waterham, H. (2006) b. Peroxisomal disorders: the single peroxisomal deficiencies. BBA. 1763, 1707-1720.
- Wang, P. and Song, C.P. (2008) Guard-cell signalling for hydrogen peroxide and abscisic acid. New Phytol. 178, 703-718.
- White, P. (2000). Calcium channels in higher plants. Biochem Biophys Acta. 171-189.
- White, P. and Broadley, M. (2003). Calcium in plants. Annals of Botany. 92, 487-511.
- Wolinski, H., Petrovic, U., Mattiazzi, M., Petschnigg, J., Heise, B., Natter, K. and Kohlwein, S.D. (2009). Imaging-based live cell yeast screen identifies novel factors involved in peroxisome assembly. J Proteome Res. 8, 20-7
- Yang, Y., Costa, A., Leonhardt, N., Siegel, R.S. and Schroeder, J.I. (2008) Isolation of a strong *Arabidopsis* guard cell promoter and its potential as a research tool. Plant Methods. 19, 4-6.
- Yang, T. and Poovaiah, B.W. (2002). Hydrogen peroxide homeostasis: activation of plant catalase by calcium/calmodulin. Proc Natl Acad Sci U S A. 99, 4097-4102.